

(NASA-TM-83908) DIFFERENTIAL SPACECRAFT  
CHARGING ON THE GEOSTATIONARY OPERATIONAL  
ENVIRONMENTAL SATELLITES (NASA) 40 p  
HC A03/MF A01 CSCI 22B

N82-26350

Unclass  
63/15 22779

# NASA

## Technical Memorandum 83908

### Differential Spacecraft Charging on the Geostationary Operational Environmental Satellites

Winfield H. Farthing  
James P. Brown  
William C. Bryant

MARCH 1982

National Aeronautics and  
Space Administration

Goddard Space Flight Center  
Greenbelt, Maryland 20771



DIFFERENTIAL SPACECRAFT CHARGING ON  
THE GEOSTATIONARY OPERATIONAL ENVIRONMENTAL SATELLITES

WINFIELD H. FARTHING

JAMES P. BROWN

WILLIAM C. BRYANT

MARCH 1982

GODDARD SPACE FLIGHT CENTER  
GREENBELT, MARYLAND 20771

## ABSTRACT

Subsystems aboard the Geostationary Operational Environmental Satellites -4 and -5 have shown numerous instances of anomalous changes in state corresponding to false commands. This paper presents evidence linking the anomalous changes to geomagnetic activity, and presumably static discharges generated by spacecraft differential charging induced by substorm particle injection events. The anomalies are shown to be correlated with individual substorms as monitored by stations of the North American Magnetometer Chain. The relative frequency of the anomalies is shown to be a function of geomagnetic activity as described by the index  $k_p$ . Finally a least squares fit to the time delay between substorm initiation and spacecraft anomaly as a function of spacecraft local time is shown to be consistent with injected electron populations with energy in the range 10 keV to 15 keV, in agreement with present understanding of the spacecraft charging mechanism. The spacecraft elements responsible for the differential charging have not been satisfactorily identified. That question is currently under investigation.

## 1. INTRODUCTION

The Geostationary Operational Environmental Satellite Program is an operational meteorological satellite program in which NASA manages the procurement, launch, and in-orbit evaluation of the satellite system and NOAA's National Earth Satellite Service (NESS) operates the system for the National Weather Service and other users. The system includes two operational satellites over the equator, one at 75° west longitude, and the other at 135° west longitude. The two satellites are identical, with the prime instrument being the Visible and Infrared Spin Scan Radiometer-Atmospheric Sounder (VAS)<sup>1</sup>.

This instrument provides day and night cloud cover imaging through eight visible and two infrared channels. East-west scan motion for the detectors is provided by the 100 rpm spin rate of the satellite, and north-south scan is provided by a single axis stepping mirror. A complete image of the earth is obtained in approximately 18.5 minutes from each satellite. Operationally, frames are initiated each half-hour.

The current systems, GOES-4 and GOES-5, are the first of the GOES satellites to also provide the capability for multispectral imaging and atmospheric sounding through which vertical profiles of water vapor content and temperature can be obtained<sup>2</sup>. This capability was incorporated as an experiment to demonstrate that sounding is of practical use on operational satellites to obtain needed information for atmospheric modeling and prediction. It has been a considerable success<sup>3</sup>, and may be incorporated by NOAA in an operational sense in the future.

In addition to the VAS, the GOES system also provides a Space Environment Monitor on each satellite<sup>4</sup>. This subsystem is comprised of a vector magnetometer, an energetic particles sensor to monitor penetrating radiation, and a solar x-ray sensor. These instruments provide part of the data base to NOAA's Space Environment Laboratories, charged with the responsibility for monitoring and providing early warning of the effects of solar-terrestrial interaction. The satellites also provide communications functions for the relay of stretched VAS data and weather facsimile (WEFAX) between earth terminals and for the collection of data from a complement of terrestrial and oceanographic data collection platforms (DCP's).

The GOES-4 and GOES-5 satellites were built for NASA by the Hughes Aircraft Company. GOES-4 was launched on September 9, 1980 and GOES-5 was launched on May 22, 1981. The GOES spacecraft all undergo an in-orbit evaluation by NASA for a period of approximately 30 days before they are turned over to NESS for operational use.

## 2. ANOMALOUS COMMANDS OBSERVED

Both GOES-4 and -5 have experienced anomalous changes of state in-orbit, primarily in the VAS subsystem. The first such changes were observed on GOES-4, March 29, 1981, when the VAS mirror which provides the north-south scan abruptly began stepping and the visible channel 6 showed an uncommanded gain step. On April 1, the mirror again began stepping when no command had been sent. Ground magnetograms from Anchorage, Alaska were examined and showed evidences of substorm activity closely correlated in time with the anomalous changes in state. The conclusion was drawn that the changes were environmentally induced, i.e., they were the instrument response to electrostatic discharges generated on the spacecraft as a result of differential charging in the local energetic electron population. The theoretical basis for such charging has been thoroughly documented<sup>5,6</sup>, and the coincidence of magnetic activity and the fact that the local time of the events was in the midnight to dawn sector provided ample grounds for this conclusion. A search for a differential charging mechanism was begun, which revealed that a portion of the VAS second stage radiation cooler was probably ungrounded. An inner member of this assembly was grounded through a wire back into the VAS electronics package. It seemed likely that the ungrounded member was charging in the environment until the breakdown potential across the insulating epoxy bond between the two members was exceeded, resulting in a large current surge flowing along the wire and into the VAS electronics package. Tests performed on the GOES-5 spacecraft, at that time awaiting launch at ETR, confirmed that the radiator was not grounded. This was corrected before launch, with the expectation that no such events would be experienced on GOES-5.

Numerous other uncommanded changes have been observed on GOES-4, and in spite of the correction made, GOES-5 has exhibited similar changes, although in different command functions. A sufficient number of events have occurred to provide a

data base for study to determine the dependence of the phenomena on magnetic activity and to determine if the events on GOES-5 are another manifestation of the same phenomena. Table 1 shows all "phantom commands" which had occurred on GOES-4 and 5 through November 23, 1981.

### 3. CORRELATION WITH GROUND MAGNETOGRAMS

Figures 1-23 show ground magnetograms of the X (north) magnetic field variation at the stations of the east-west chain of the North American Magnetometer Network sponsored by the National Science Foundation<sup>7</sup>. These stations transmit through the data collection platform system on GOES to the NOAA Space Environment Laboratories, where the data processing and display functions are performed. Each figure is labelled with the GOES spacecraft ID at the time of a corresponding command anomaly. A substorm observed on these traces appears as a more or less short lived depression or enhancement of the X component depending on whether the observing station is east or west of the Harang discontinuity which separates the eastward, pre-midnight electrojet from the westward, post-midnight electrojet<sup>8</sup>. The most prominent signature is a depression, or "magnetic bay", under westward flowing electrojet activity. At times of world wide magnetic storms, enhanced electrojet activity persists for periods of one to several days, and is accompanied by a sustained world wide depression of the horizontal field at mid latitude stations. Table 2 gives the geographic and geomagnetic (dipole) coordinates of the stations used in these figures. The position of the electrojet in latitude is strongly dependent on local time and on magnetic activity. The stations used in the east-west chain are well situated for monitoring the electrojet in the nighttime hours and during periods of moderate magnetic activity.

Anchorage is not formally a part of the North American Chain. Its southerly location places it out of the region of electrojet activity much of the time. Its traces often are more similar to mid latitude behaviour of the magnetic field.

For GOES-4, there are 13 events displayed. In 8 of these the command anomaly occurs within four hours of the onset of a well defined substorm (Figures 1,3, 5, 6, 7, 10, and two events in Figure 2). In the remaining 5 there is

significant sustained storm or substorm activity so that it is not possible to associate a particular substorm as correlated with the anomaly. Substorm activity is believed to be invariably associated with the injection of a hot rarified plasma into the magnetosphere in the vicinity of local midnight and the depletion in the morning quadrant of the relatively cold and dense plasma found there in quiet times<sup>9</sup>. Motion of the injected particles is dependent on their energy and charge, and on the magnetic field configuration. Energetic electrons drift eastward toward dawn, overtaking the slower moving synchronous altitude satellites in their path. The drift rate is energy dependent, so that the leading edge of the cloud contains the most energetic of the particles injected during the substorm. If the intensity of the electron flux is sufficient, shadowed portions of the spacecraft may charge to a potential approaching the thermal energy of the electrons. This model explains why spacecraft charging should occur in the postmidnight sector, and indeed all of the anomalous commands which have occurred on GOES-4 and GOES-5 have been in that general local time sector. Two events occurred just prior to local midnight and one event occurred at 07:01 local time.

For GOES-5, 13 events are displayed in the magnetograms. While the correlation between the events and well defined substorms is not as striking, it is still possible to select 8 events in which a well defined substorm is present (Figures 12,14,15,19,20,21, and two events in Figure 17). In Figures 13 and 22, the lack of a definite correlation may be a result of the station location. These events both occurred when the satellite was near local midnight. The stations of the magnetometer chain were at that time at magnetic local times from 2.6 to 6.5 hours earlier, placing them under the eastward flowing electrojet west of the Harang discontinuity. Since there is no east-west current continuity at the Harang discontinuity, it is not surprising that the substorm signature is not detected there for these two events. The same effect shows up in several of the other magnetograms. In Figure 12, the surge of westward current responsible for the signature at the eastern stations is not detected at College, placing the Harang discontinuity between 22:30 hours and 23:50 hours in local time. A small positive signature in D is observed at College (not shown). This is possibly indicative of an outward flowing, field aligned filament north of College. In Figure 17, two substorms occurred, one at 6:45 UT which was detected only at Lynn Lake, and another at 7:50 UT., which was also detected at Fort Simpson and

Norman Wells. The latter stations had by that time rotated through the Harang discontinuity and were under the westward electrojet. Both substorms resulted in charging events on GOES-5.

#### 4. CORRELATION WITH MAGNETIC INDEX KP

A more quantitative basis for determining the relationship between magnetic activity and the occurrence of anomalous commands can be obtained by tabulating the magnetospheric index  $k_p$  and the times of anomaly occurrence. These data are shown in tables 3, 4, and 5 for GOES-4 in the month of April 1981. The magnetic index  $k_p$  is a logarithmic index of worldwide magnetic activity on a scale of 0 to 9. It is determined for each 3 hour period in each UT day. The entries in Table 3 show the number of days of the month in which the time sector (row) had the given value of  $k_p$  (column). Table 4 shows the occurrence of anomalous commands tabulated in the same way. Table 5 shows the ratio of corresponding elements in Table 4 to those in Table 3, and can be thought of as an estimator of the probability of a command anomaly given that time sector and value of  $k_p$ .

The local time for GOES-4, at  $135^\circ$  west longitude, is 9 hours earlier than UT. Thus the time interval tabulated covers 2100 LT to 0600 -LT. Note that the two events which occurred prior to local midnight were both within 1/2 hour of midnight. On the right hand margin of table 5 is computed the marginal distribution of anomalies with local time, showing that the events occur in the time sector from just before midnight to dawn. More importantly the lower margin displays the marginal distribution with  $k_p$ . While the number of observations for  $k_p$  less than 1 and greater than or equal to 6 is too small to be significant, the remainder of the classes show a clear correlation of relative frequency with  $k_p$ .

Tables 6, 7, and 8 show the same data for GOES-5 except that the months of August, September, and October have been combined to obtain a sufficient number of events to study.

In the GOES-5 case the local time span is from 2200 LT to 0700 LT. The one event that occurred before midnight was at 23:20 LT. The marginal distribution of anomalies with  $k_p$  again shows a strong correlation. The distributions for



both GOES-4 and GOES-5 are graphed in Figure 24.

Because of the differences in the time base, one cannot compare the magnitude of relative frequencies between GOES-4 and GOES-5. Further, the relative frequency for GOES-4 is understated, since the most susceptible command function, the "stepscan on", will go undetected when the mirror is already stepping, roughly 67 percent of the time. Only one anomaly was observed on GOES-4 in the months of August through October. This fact is more likely an indication of a change in susceptibility of the satellite, the generally lower level of magnetic activity in those months, and the "blindness" of GOES-4 when the mirror is stepping than it is an indication of a seasonal effect. Four additional command anomalies on GOES-4 and seven additional anomalies on GOES-5 occurred through February 2, 1982. These events have not been included in the analysis. It is clear that the events on both spacecraft are correlated with magnetic activity. While this correlation shows that the anomalies are environmentally related, it does not follow automatically that spacecraft charging is the mechanism. However, the dependence on local time, magnetic activity, and the correlation with individual substorm activity together force the conclusion of spacecraft charging in the absence of any other viable explanation.

##### 5. PLASMA DRIFT VELOCITY

The rationale for the spacecraft charging phenomena given in section 3 predicts that there will be a time delay between the injection of plasma in the midnight sector and the arrival of the energetic electrons at the satellite. This prediction is verified by study of those events on GOES-4 and GOES 5 which are associated with well defined substorms, as listed in section 3. Measuring the time delay between substorm initiation and the event at the spacecraft produces the scatter diagram of Figure 25. The best least squares fit to the data is

$$y = 0.332x + 22.46$$

where  $y$  is the period in minutes required for the particles to drift to the local time  $x$ , also in minutes. For the typical cloud represented by this fit the time required to drift completely around the earth is  $0.332(24)(60) = 478$  minutes. Use of Figures 1.2 and 1.3 from Van Allen (1962)<sup>10</sup> results in electron

energy of slightly greater than 10 keV if the particles are mirroring at dipole latitude of  $90^{\circ}$ , or slightly greater than 15 keV if they are mirroring at the geomagnetic equator. These energies are very close to those which have been measured in situ during injection events. Note that dipole latitudes near  $90^{\circ}$  cannot be accessed because of the presence of the earth and its atmosphere.

The derivation of a typical dispersion relationship implicitly assumes that the particles are injected at a point source in the magnetosphere and that the time required for the spacecraft to charge is negligible compared to the drift time to the satellite. The effect of the first assumption is to bias the measurements of drift time in Figure 25 negatively independent of local time. The effect of the second assumption is to bias the measurements positively, and is probably less important because of the energy selection involved in the drift process. The interesting observation is made that the point of origin of the clouds appears from Figure 25 to be the eastern edge of the Harang discontinuity, which is known to be intimately involved in the substorm mechanism<sup>11</sup>. The biases are such that the true point of origin may well be at the center of the Harang discontinuity. The complex processes that occur in the ionosphere and magnetosphere along magnetic field lines that intersect the earth at the Harang discontinuity remain to be fully understood.

## 6. CONCLUSION

The potential for problems resulting from spacecraft differential charging has received much attention since the phenomenon was first identified. Although this has resulted in much more care being exercised in the structural grounding and external surface treatment of scientific and operational spacecraft, the charging phenomenon remains a persistent problem in a region of space increasingly utilized by weather and communications satellites. The same region is considered for future use by applications requiring large structural systems, for which the effects of the plasma population have not been tested. Such effects are indeed the most important environmental effect on private and government spacecraft systems, next to the sun. The operational meteorological satellite would provide an excellent platform for monitoring this environment, having the advantage over scientific satellites of a continuing ground data

acquisition capability and essentially 100 percent coverage in orbit. GOES East and GOES West together could provide complete coverage for the considerable array of communications satellites situated between them, as a result of the propagation effects discussed in section 3 and demonstrated in section 5. The European Space Agency (ESA) has already incorporated a low energy particle monitor on Meteosat-2 as well as an electrostatic event detector, having experienced a large number of anomalies on Meteosat-1 attributed to spacecraft charging. It can be seen that the potential exists for worldwide, continuous monitoring of these effects through judicious international cooperation within the already existing weather satellite network.

The present Space Environment Monitor on GOES does not include the capability for monitoring particle populations of energies responsible for spacecraft charging. The requirements were set for GOES before the charging was recognized. Addition of the instrument necessary has been identified by NOAA's Space Environment Laboratories as a high priority for future operational satellites. Unfortunately present programmatic and funding limitations will likely prevent the addition of this capability until the late 1990's.

## ACKNOWLEDGEMENTS

Appreciation is due Mr. Charles Hornback and other personnel of the forecast center of the Space Environment Laboratories, Boulder, Colorado for the magnetograms which form the data base for this study. Appreciation is expressed to Dr. J. P. Heppner for his review of and helpful comments on the paper.

## REFERENCES

1. Santa Barbara Research Center: Final Report, Visible Infrared Spin Scan Radiometer-Atmospheric Sounder (VAS). Report to NASA under contract NAS5-20769 from Santa Barbara Research Center, Santa Barbara, California. August, 1980.
2. Suomi, V., T. Vonder Haar, R. Krauss, and A. Stamm: "Possibilities for Sounding the Atmosphere from a Geosynchronous Spacecraft", Space Research, XI, 609, 1971.
3. Smith, W. L. et al: "First Sounding Results from VAS-D", Bulletin American Meteorological Society, 62, 232, 1981..
4. Grubb, R. N.: "The SMS/GOES Space Environment Monitor Subsystem", NOAA Technical Memorandum. ERL SEL-43. December, 1975.
5. Deforest, Sherman E.: "Spacecraft Charging at Synchronous Orbit," J. Geophys. Res., 27, 651, 1972.
6. Rosen, Alan: "Large Discharges and Arcs on Spacecraft", Astronautics and Aeronautics, 13, June, 1975.
7. Lanzerotti, L. J., R. D. Regan, M. Sugiura, and D. J. Williams: "Magnetosphere Networks During the International Magnetosphere Study, Eos Trans. AGU, 57, 442, 1976.
8. Harang, L.: Terr. Mag., 51, 353, 1946.
9. Deforest, S. E. and C. E. McIlwain: "Plasma Clouds in the Magnetosphere", J. Geophys. Res., 26, 3587, 1976.
10. Van Allen, James A: "Dynamics, Composition and Origin of the Geomagnetically - Trapped Corpuscular Radiation", Trans. Int. Astron. Union, 11B, 99, 1962.
11. Akasofu, S. I.: Physics of Magnetospheric Substorms, p. 414, D. Reidel Publishing Co. Dordrecht, Holland (1978).

TABLE 1 - GUES -4 AND -5  
PHANTOM COMMANDS

DATE	S/C	TIME UT	ECLIPSE TIME UT	COMMAND NUMBER	TO PRODUCE ANOMALY NAME
3/29/81	G-4	1142	0832 to 0937 Ch. 6 gain step.	331/334 and 302	Step Scan ON (primary or redundant cmd) Visible
4/1/81	G-4	09:55:31	0833 to 0934	331/334	Step Scan ON (primary or redundant cmd).
4/1/81	G-4	10:10:22	0833 to 0934	331/334 and 302	Step Scan ON (primary or redundant cmd) Visible Ch. 6 gain step.
4/13/81	G-4	09:03:17	No eclipse	331/334	Step Scan ON (primary or redundant cmd)
4/14/81	G-4	11:36:35	No eclipse	331/334	Step Scan ON (primary or redundant cmd)
4/17/81	G-4	08:38:22	No eclipse	331/334	Step Scan ON (primary or redundant cmd)
4/19/81	G-4	12:35:22	No eclipse	331/334	Step Scan ON (primary or redundant cmd)
4/20/81	G-4	14:35:22	No eclipse	331/334	Step Scan ON (primary or redundant cmd)
4/21/81	G-4	14:45:44	No eclipse	030	VDM half resolution
4/24/81	G-4	09:40:33	No eclipse	331/334	Step Scan ON (primary or redundant cmd)
4/26/81	G-4	08:36:27	No eclipse	331/334	Step Scan ON (primary or redundant cmd)
8/20/81	G-5	08:21:58	No eclipse	301	Ch. 7 gain step (from 2 to 3)
8/23/81	G-5	11:08:05	No eclipse	301	Ch. 7 gain step (from 2 to 3)
8/28/81	G-5	05:20:39	No eclipse	301	Ch. 7 gain step (from 2 to 3)
8/29/81	G-5	10:17:01	No eclipse	301	Ch. 7 gain step (from 2 to 3)

TABLE 1 (CONT)

DATE	S/C	TIME UT	ECLIPSE TIME UT	NUMBER	COMMAND TO PRODUCE ANOMALY NAME
9/11/81	G-5	12:01:39	0426-0527	301	Ch. 7 gain step (from 2 to 3)
9/12/81	G-5	10:47:33	0425-0527	301	Ch. 7 gain step (from 2 to 3)
10/2/81	G-4	14:49:41	0819-0923	030	VDM half resolution
10/10/81	G-5	07:11:03	0421-0511	301	Ch. 7 gain step (from 2 to 3)
10/10/81	G-5	08:35:55	0421-0511	301	Ch. 7 gain step (from 2 to 3)
10/11/81	G-5	07:46:22	0423-0510	301	Ch. 7 gain step (from 2 to 3)
10/12/81	G-5	08:57:35	0425-0507	301	Ch. 7 gain step (from 2 to 3)
10/21/81	G-5	09:14	None	301	Ch. 7 gain step (from 2 to 3)
11/12/81	G-5	10:58	None	301	Ch. 7 gain step (from 2 to 3)
11/22/81	G-5	06:46:11	None	301	Ch. 7 gain step (from 2 to 3)
11/23/81	G-5	10:58:36	None	301	Ch. 7 gain step (from 2 to 3)
11/23/81	G-4	12:10:16	None	331/334	Step Scan On

TABLE 2 Stations and Locations of East-West Chain

Station	Code Name	Geographic Latitude	Geographic Longitude	Geomagnetic Latitude
Lynn Lake	LYN	56°51'	-101°04'	65.96°
Fort Smith	ESM	60°00'	-112°00'	67.26°
Fort Simpson	FSP	61°45'	-121°14'	67.20°
Norman Wells	NOW	65°02'	-127°00'	69.35°
College	COL	64°53'	-148°03'	64.76°
Anchorage	ANC	61°12'	-149°56'	61.3



TABLE 3  
APRIL KP

time UT	kp												
	0	1-	1	2-	2	3-	3	4-	4	5-	5	6-	>6
6-9	2		6		6		5		3		6		2
9-12	1		3		9		6		7		4		0
12-15	0		5		5		8		5		3		4

TABLE 4  
GOES-4 ANOMALIES APRIL

time UT	kp	0	1-	1	2-	2	3-	3	4-	4	5-	5	6-	>6
6-9											1		1	
9-12								1			2		2	
12-15											1		2	

TABLE 5  
GOES-4 RELATIVE FREQUENCY APRIL

time UT	kp	0	1-	1	2-	2	3-	3	4-	4	5-	5	6-	>6
6-9		0/2		0/6		0/6		0/5		1/3		1/6	0/2	2/30
9-12		0/1		0/3		0/9		1/6		2/7		2/4	-	5/30
12-15		-		0/5		0/5		0/8		1/5		2/3	0/4	3/30
		0/3		0/14		0/20		1/19		4/15		5/13	0/6	

TABLE 6  
AUGUST THROUGH OCTOBER kp

time UT	kp	0	1-	1	2-	2	3-	3	4-	4	5-	5	6-	>6
3-6.		6		18		25		24		14		3		2
6-9		5		21		22		27		10		6		1
9-12		3		19		29		26		7		8		0

TABLE 7  
GOES-5 ANOMALIES, AUGUST THROUGH OCTOBER

time UT	kp												
	0	1-	1	2-	2	3-	3	4-	4	5-	5	6-	>6
3-6							1						
6-9					1		2		1		1		
9-12					1		1		2		1		

TABLE 8  
GOES-5 RELATIVE FREQUENCY AUGUST THROUGH OCTOBER

time UT	kp													
	0	1-	1	2-	2	3-	3	4-	4	5-	5	6-	>6	
3-6	0/6		0/18		0/25		1/24		0/14		0/3		0/2	1/92
6-9	0/5		0/21		1/22		2/27		1/10		1/6		0/1	5/92
9-12	0/3		0/19		1/29		1/26		2/7		1/8		0/0	5/92
	0/14		0/58		2/76		4/77		3/31		2/17		0/3	

START TIME: 1981 0809=0329 0000  
EAST-NEST CHAIN X TRACE

TOTAL SCALE IS 5000 GAMMA

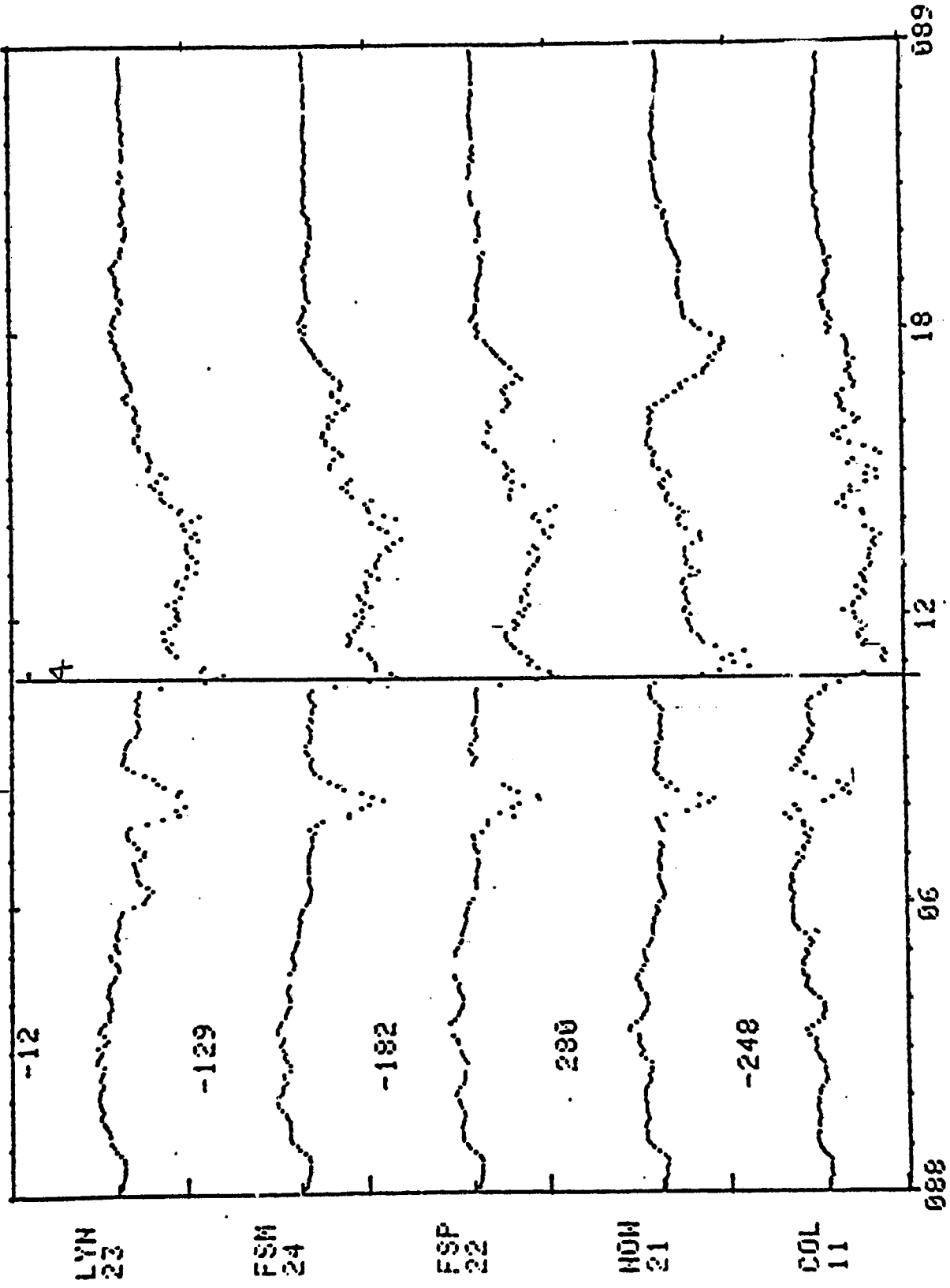


FIGURE 1

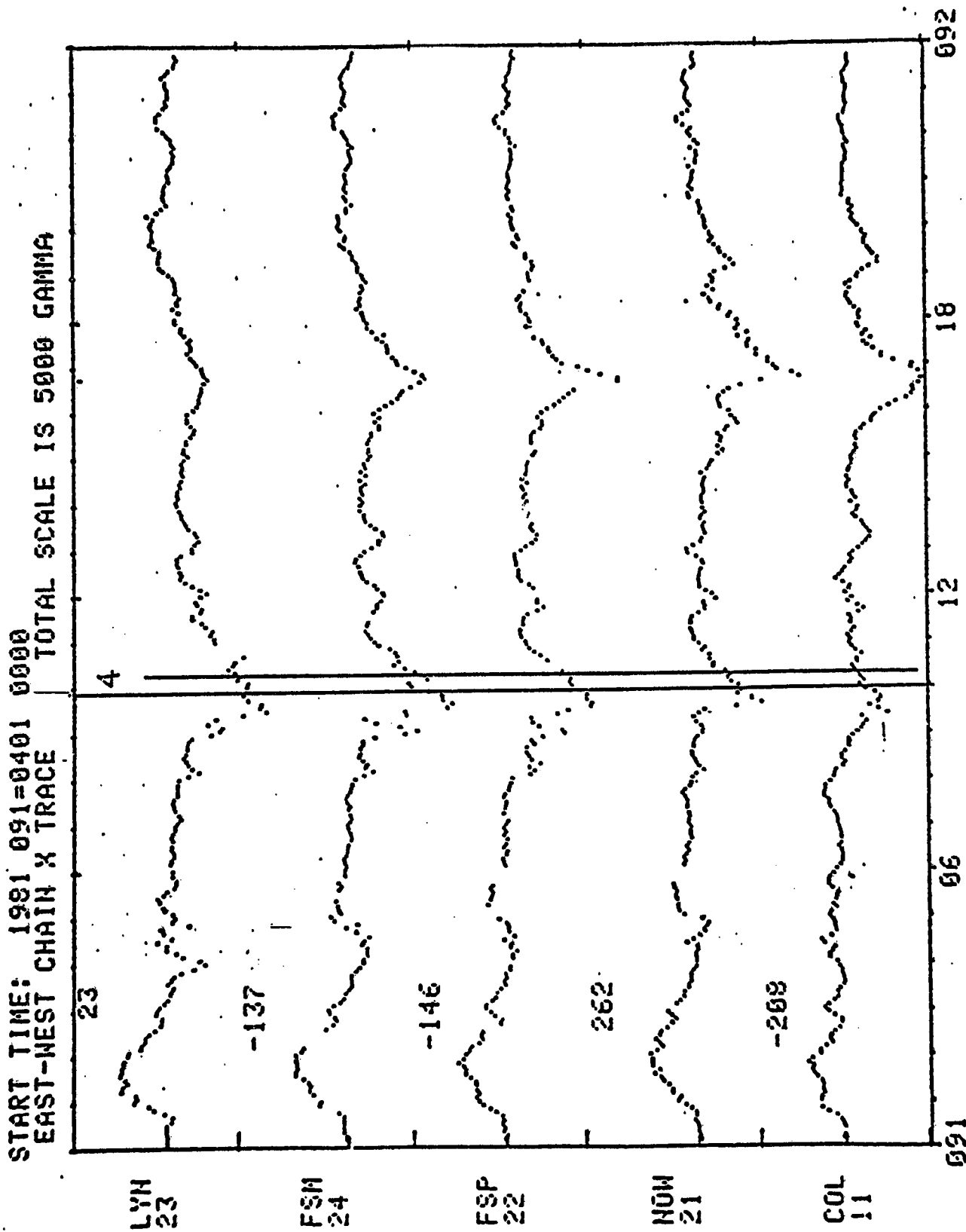


FIGURE 2



START TIME: 1981 103=0413 0000 TOTAL SCALE IS 5000 GAMMA  
EAST-NEST CHAIN X TRACE

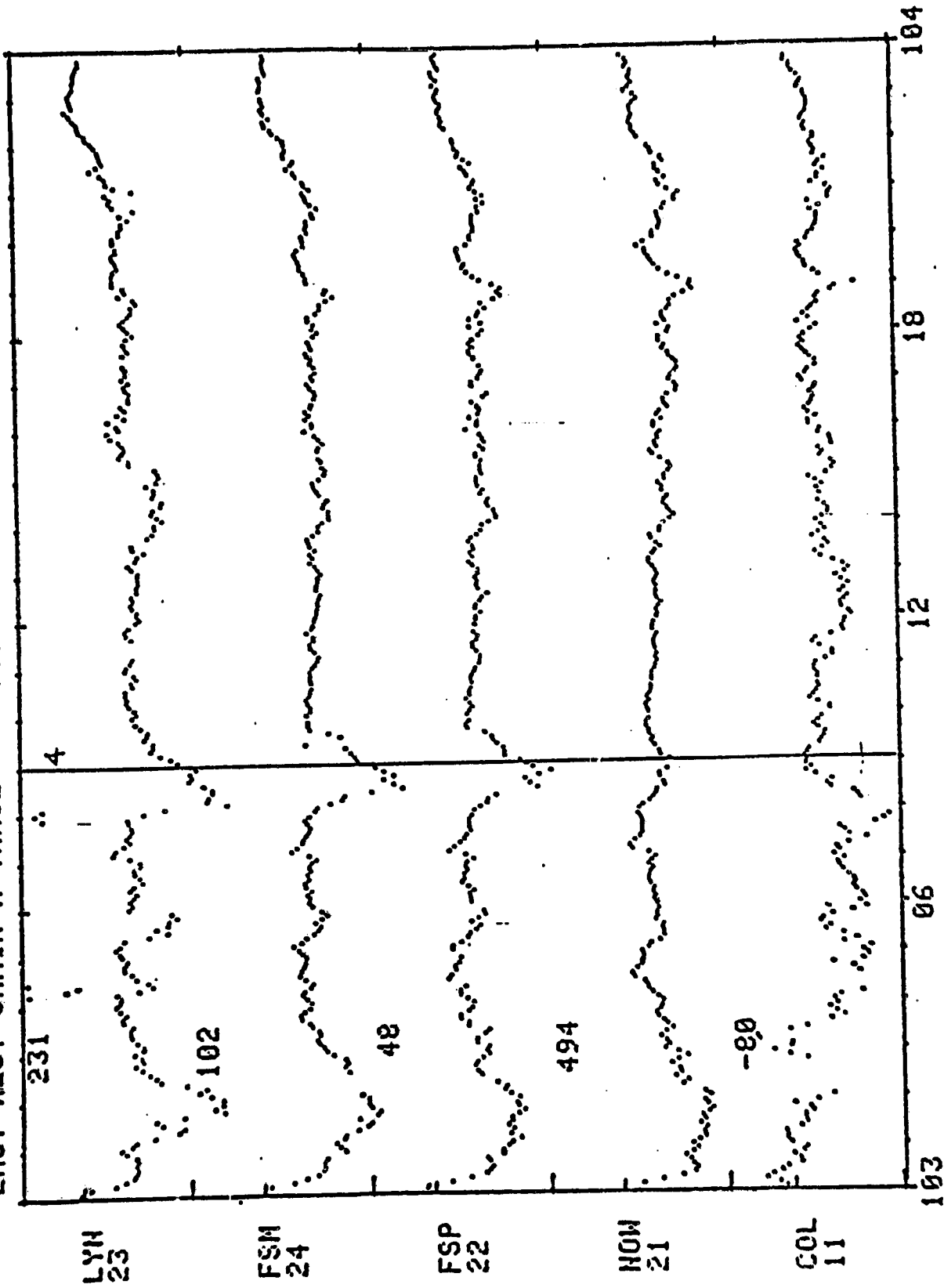


FIGURE 3

ORIGINAL PAGE IS  
OF POOR QUALITY

START TIME: 1981 104=0414 0000  
EAST-NEST CHAIN X TRACE TOTAL SCALE IS 5000 GAMMA

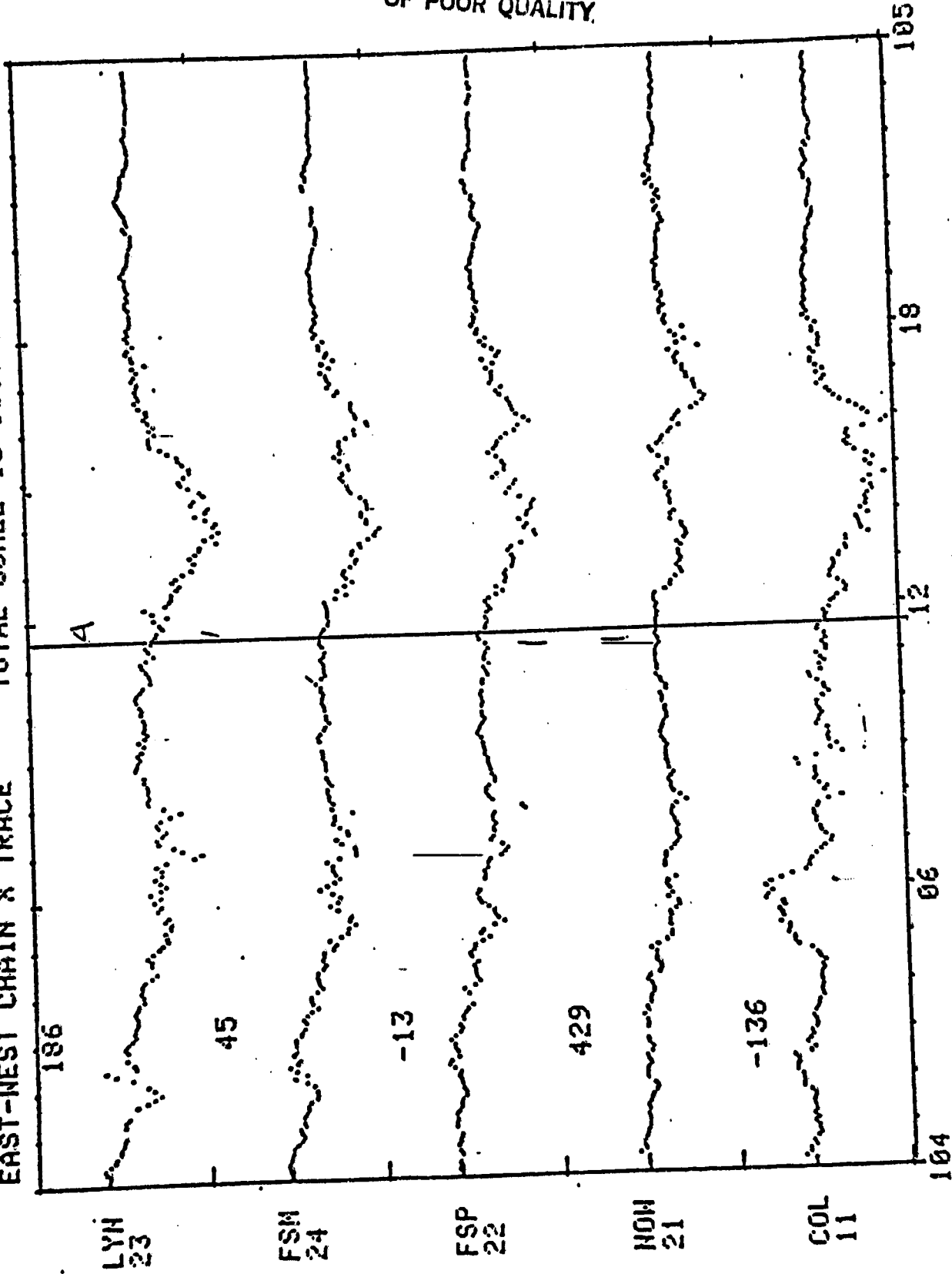


FIGURE 4

START TIME: 1981 107=0417 0000  
EAST-NEST CHAIN X TRACE TOTAL SCALE IS 5000 GAMMA

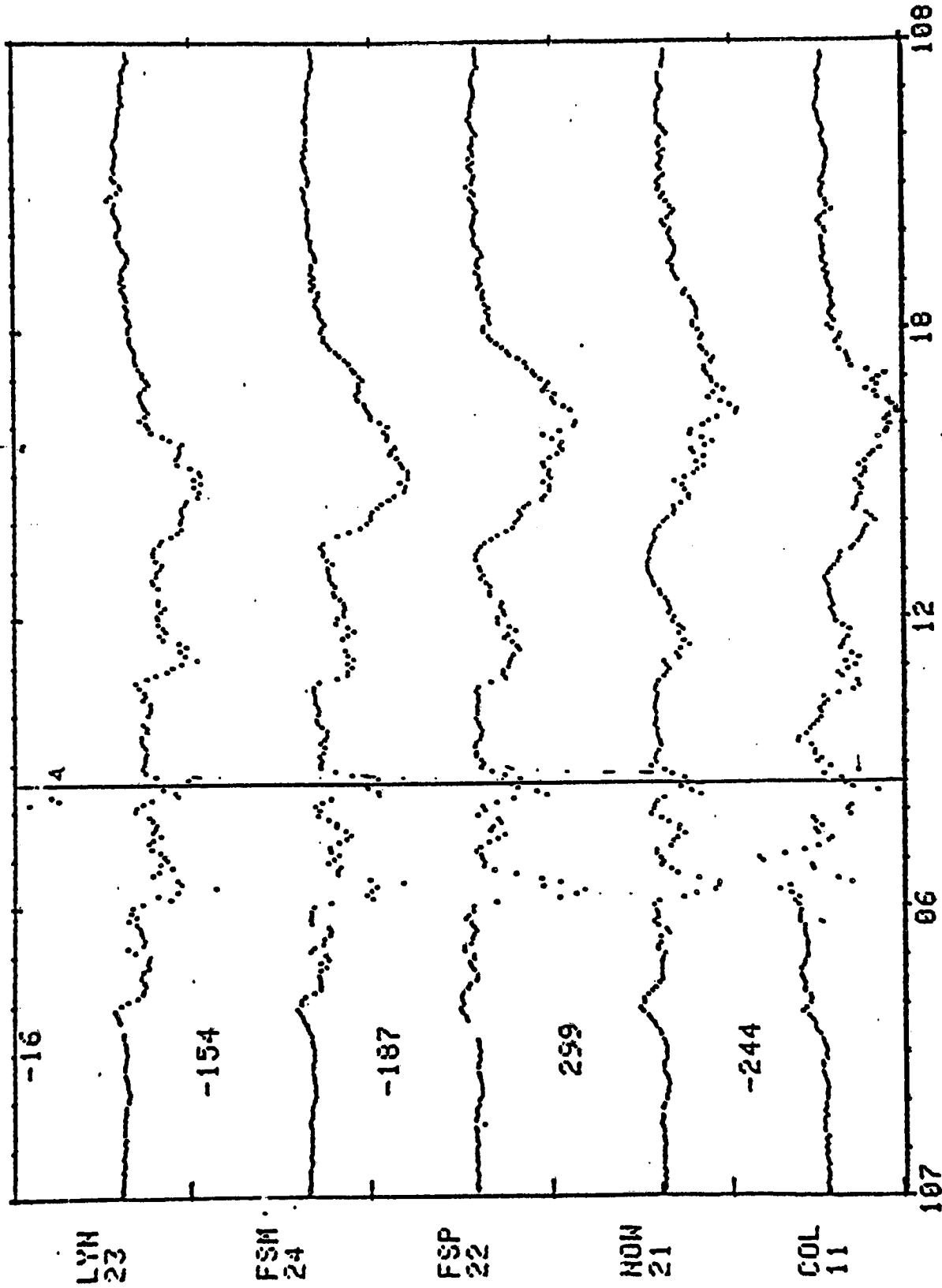


FIGURE 5

ORIGINAL PAGE IS  
OF POOR QUALITY

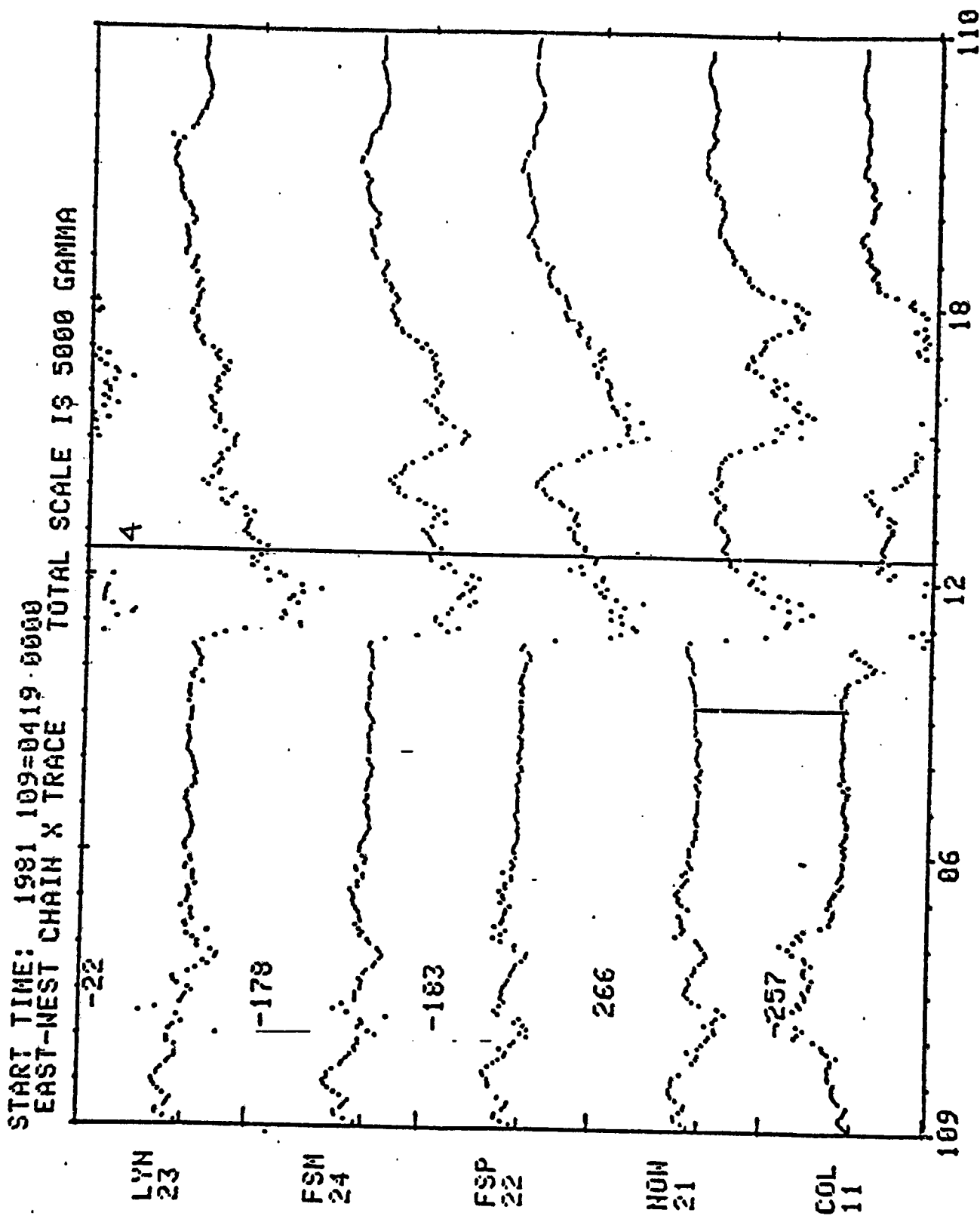


FIGURE 6

START TIME: 1981 110=0420 0000  
EAST-NEST CHAIN X TRACE TOTAL SCALE IS 5000 GAMMA

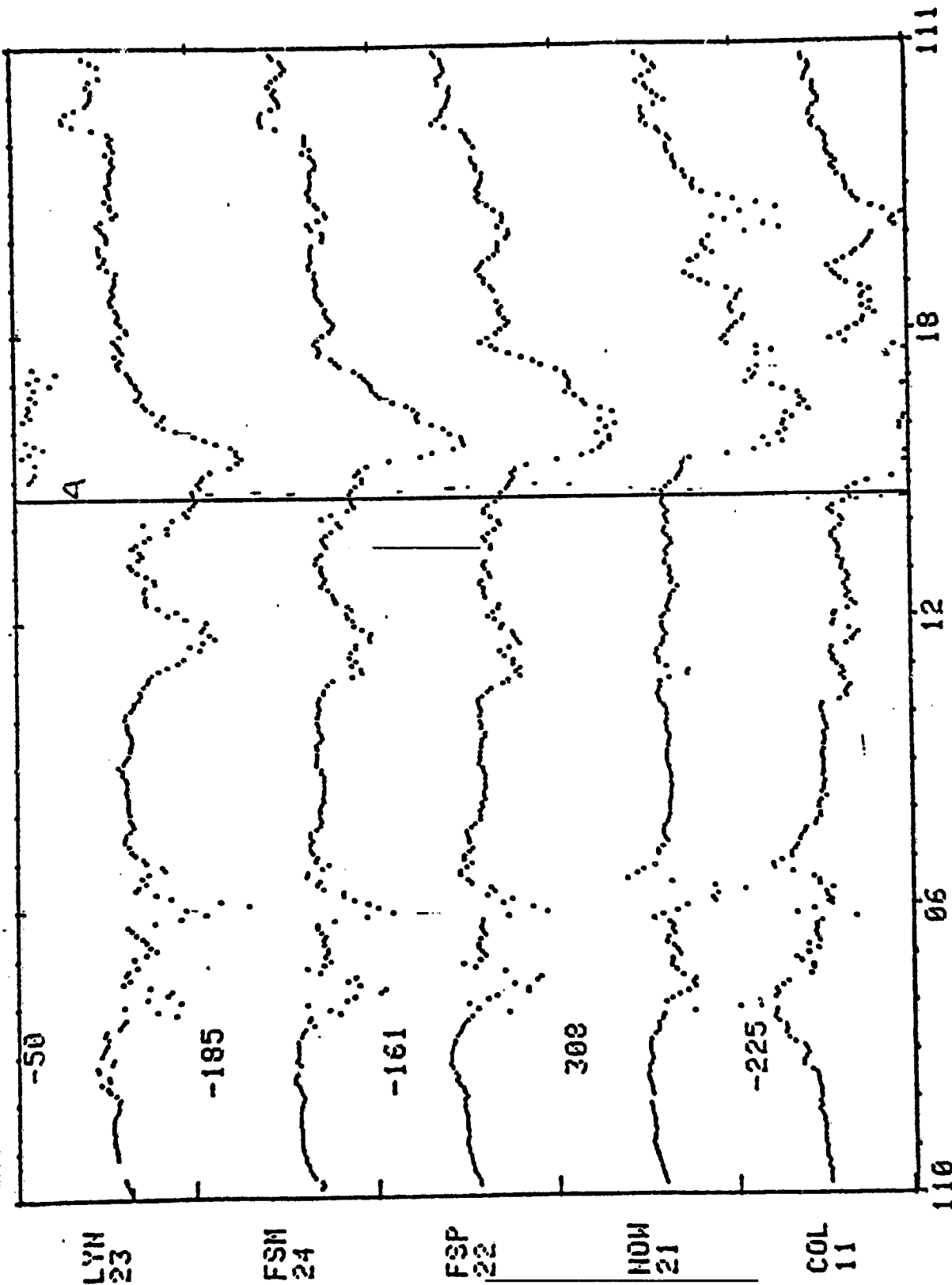


FIGURE 7

ORIGINAL FILE IS  
OF POOR QUALITY

START TIME: 1981 111=0421 0000  
EAST-NEST CHAIN X TRACE TOTAL SCALE IS 5000 GAMMA

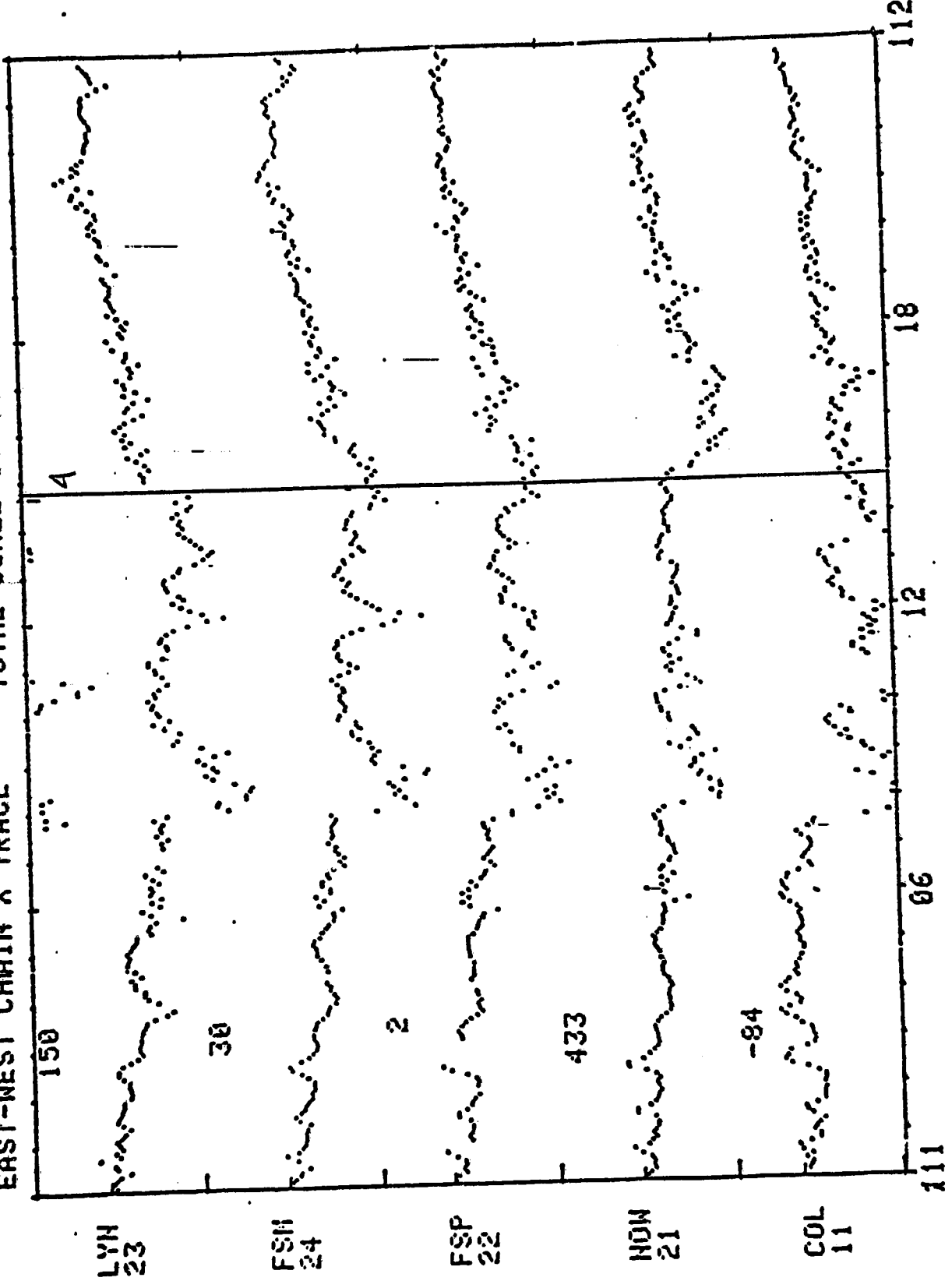


FIGURE 8

ORIGINAL PAGE IS  
OF POOR QUALITY

START TIME: 1981 114=0424 0000  
EAST-NEST CHAIN X TRACE TOTAL SCALE IS 5000 GAMMA

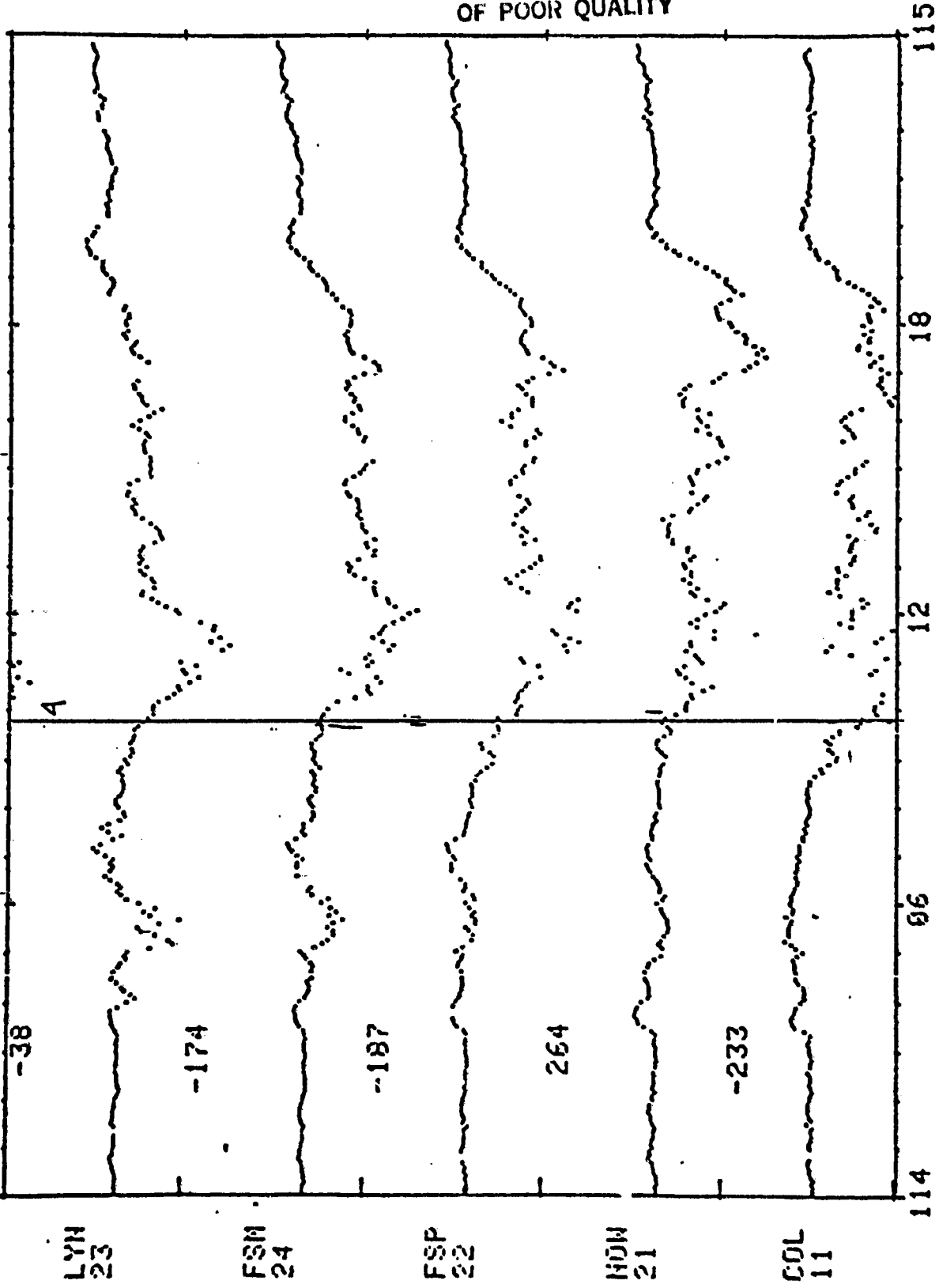


FIGURE 9

ORIGINAL PAGE IS  
OF POOR QUALITY

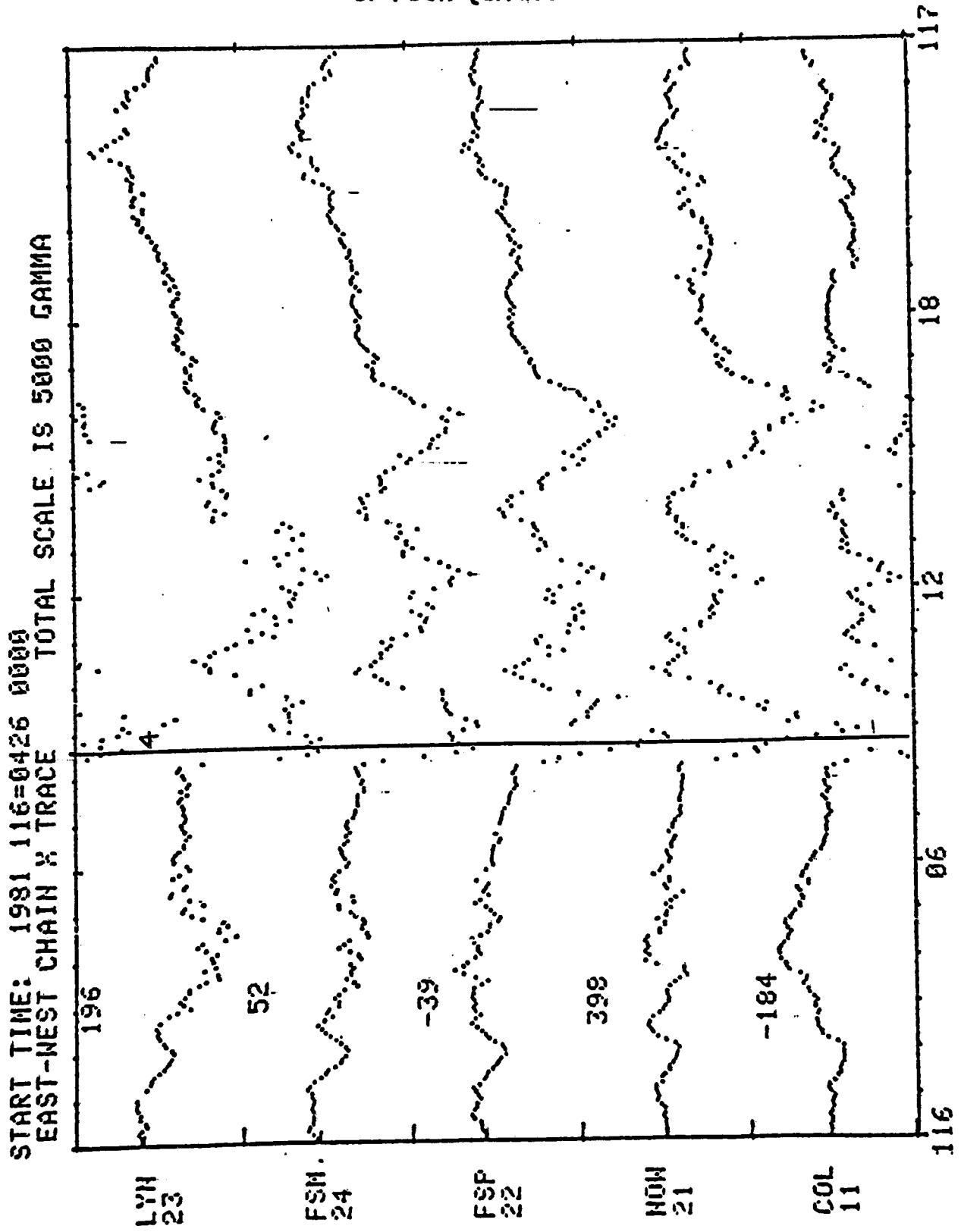


FIGURE 10



START TIME: 1981 276=1003 0000  
EAST-NEST CHAIN X TRACE TOTAL SCALE IS 5000 GAMMA

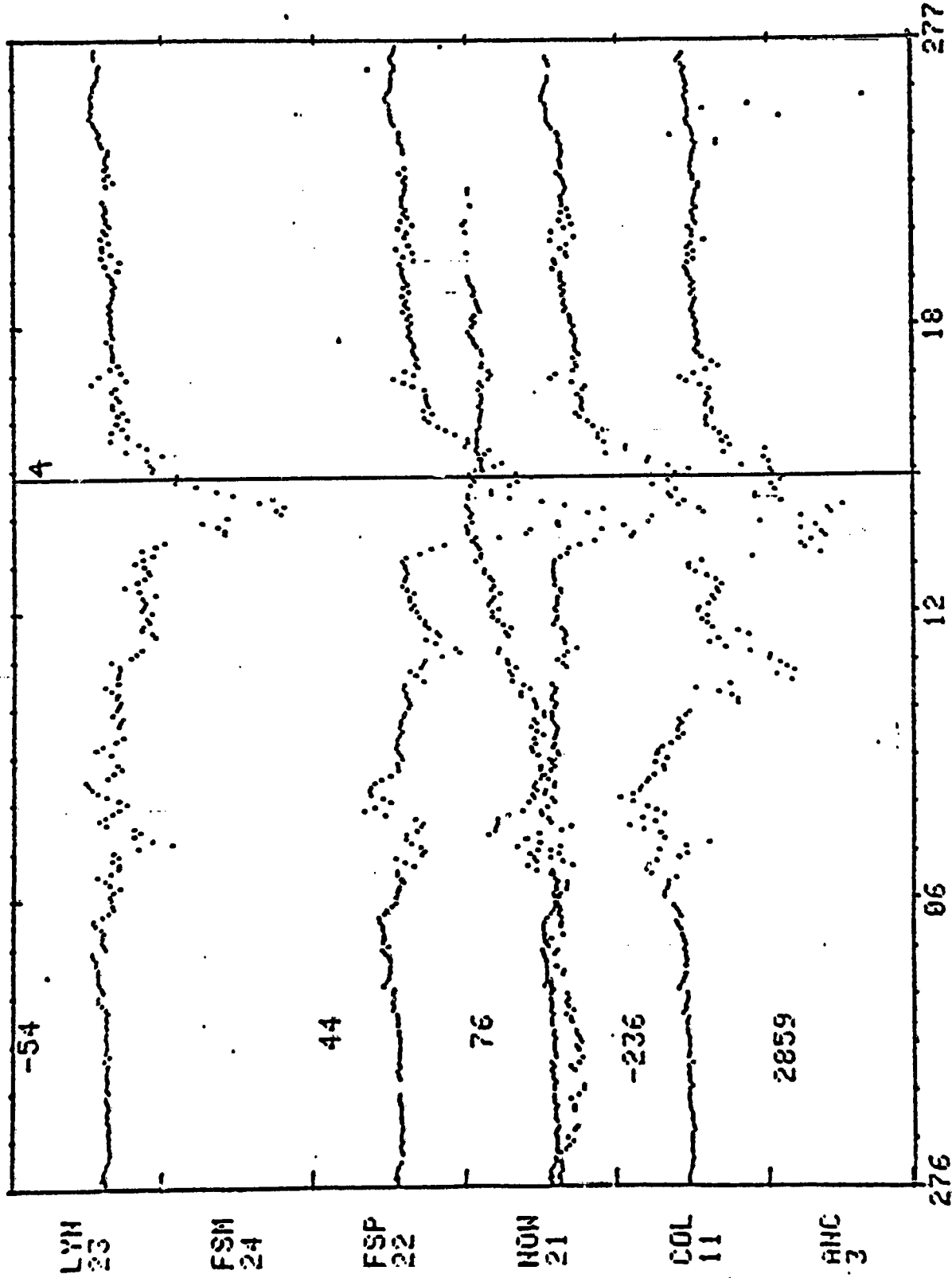


FIGURE 11

START TIME: 1981 232=0920 0000  
EAST-NEST CHAIN X TRACE TOTAL SCALE IS 5000 GAMMA

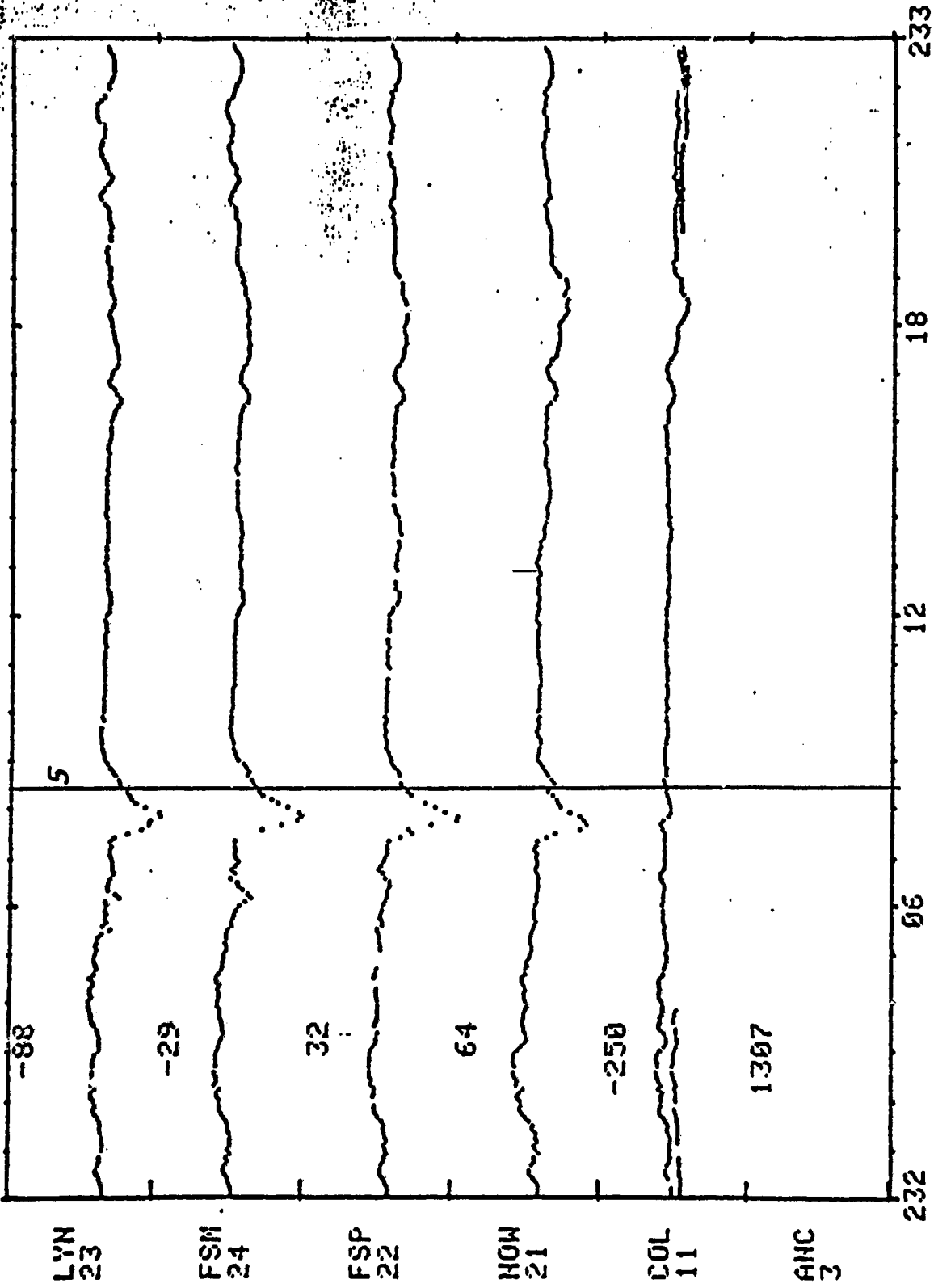


FIGURE 12

ORIGINAL PAGE IS  
OF POOR QUALITY

START TIME: 1981 240=0928 0000  
EAST-WEST CHAIN X TRACE TOTAL SCALE IS 50000 GAMMA

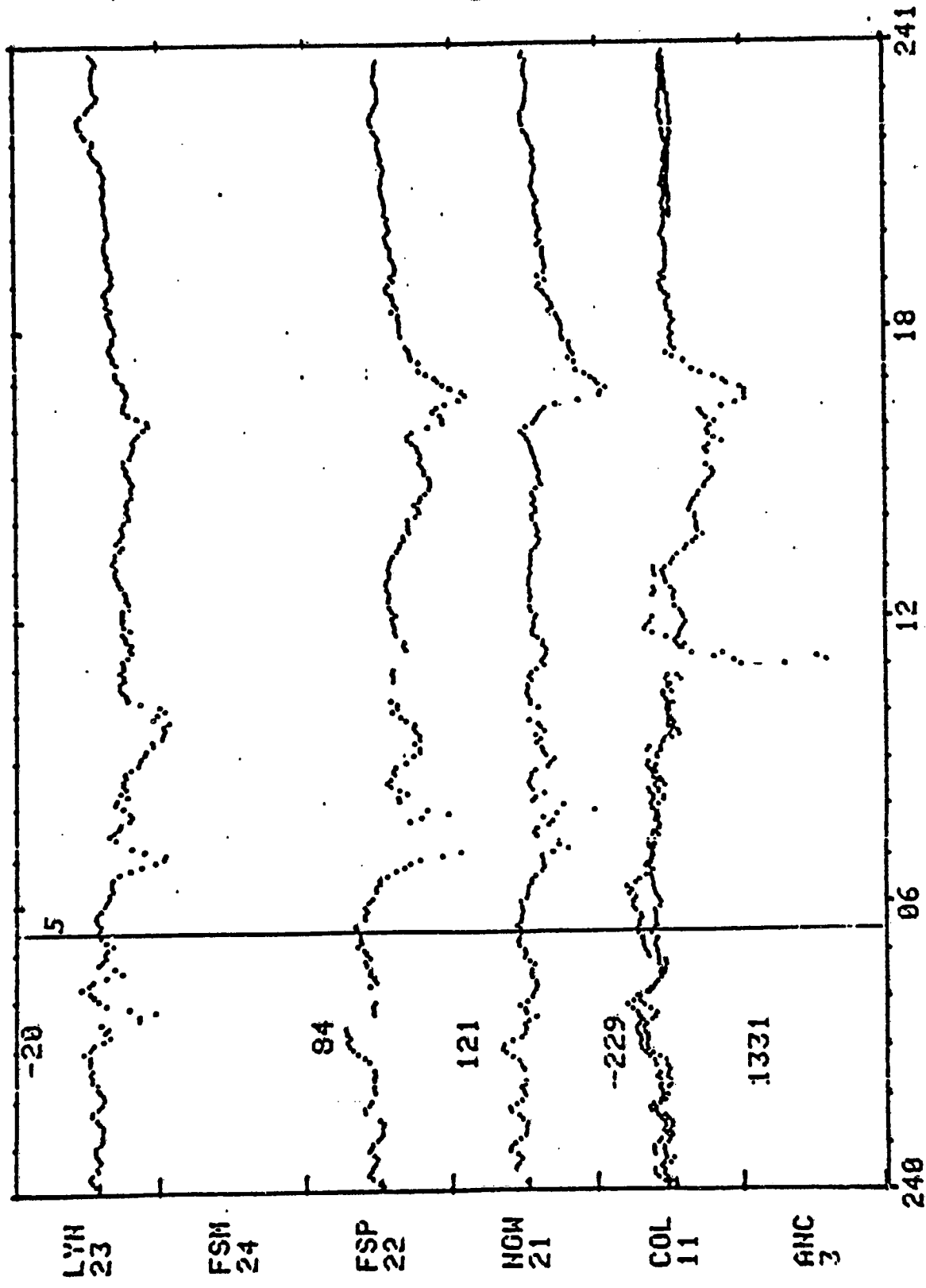


FIGURE 13

START TIME: 1981 241=0829 0000  
EAST-WEST CHAIN X TRACE TOTAL SCALE IS 5000 GAMMA

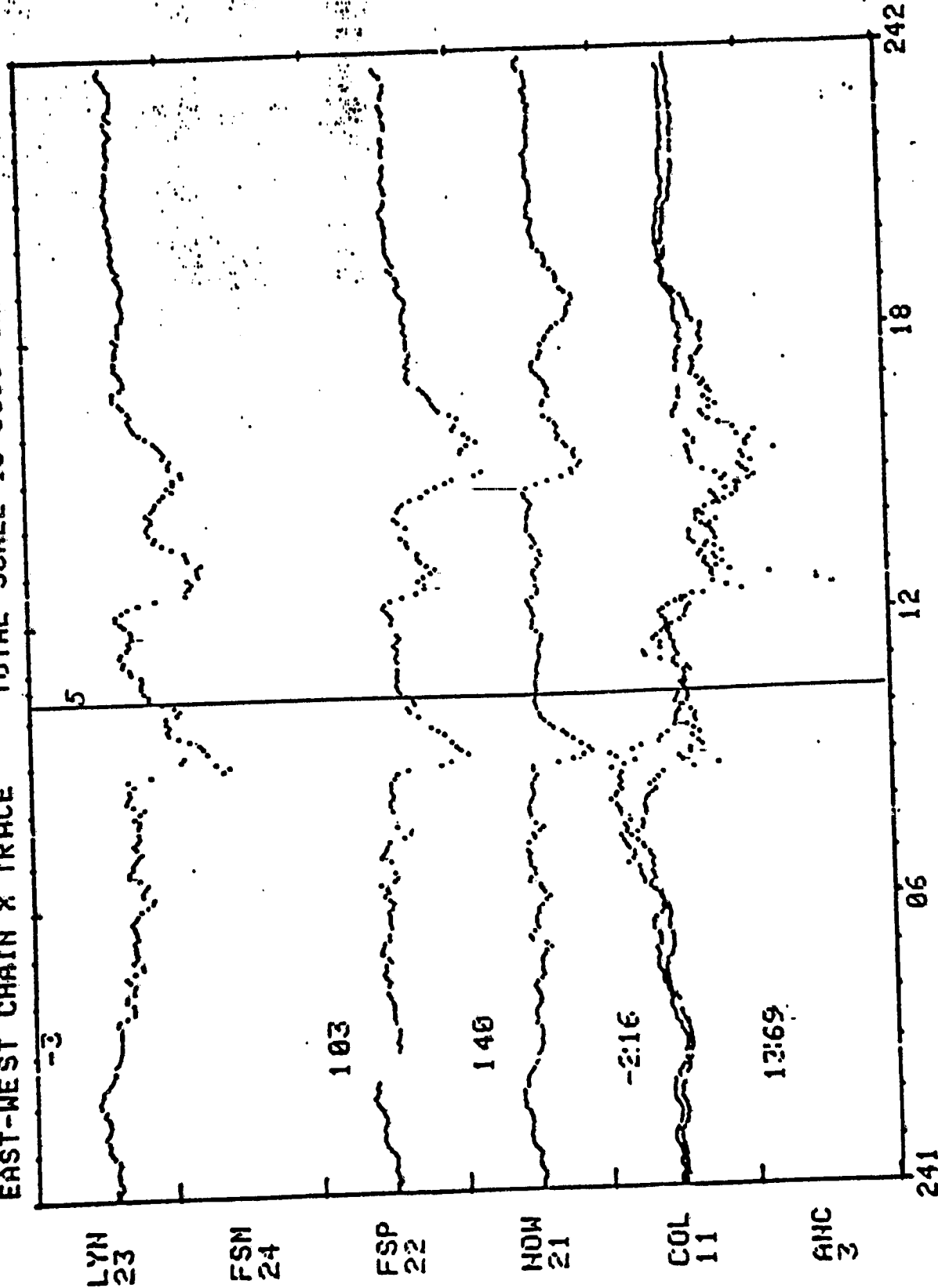


FIGURE 14

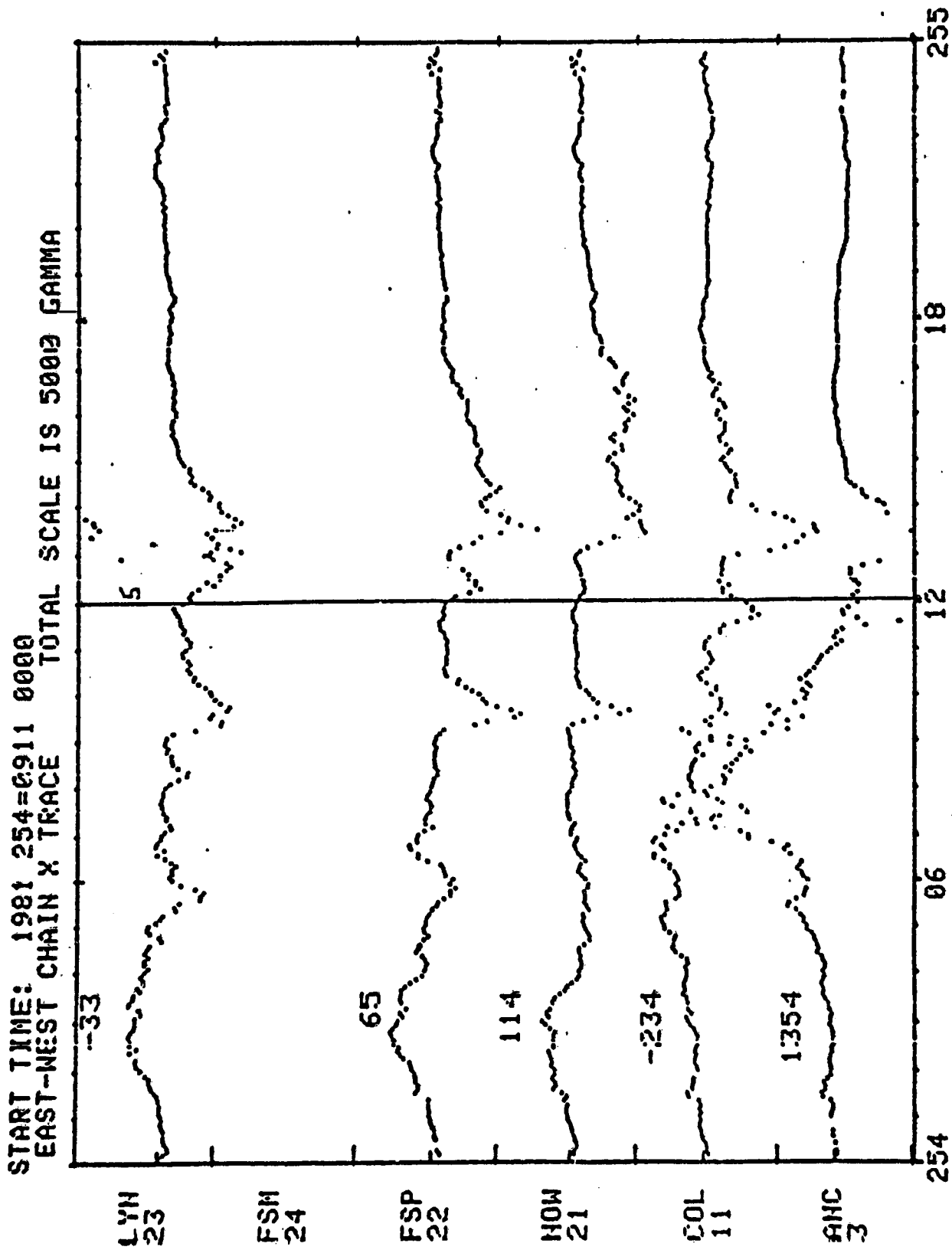


FIGURE 15

START TIME: 1981 255=0912 0000  
EAST-WEST CHAIN X TRACE TOTAL SCALE IS 5000 GAMMA

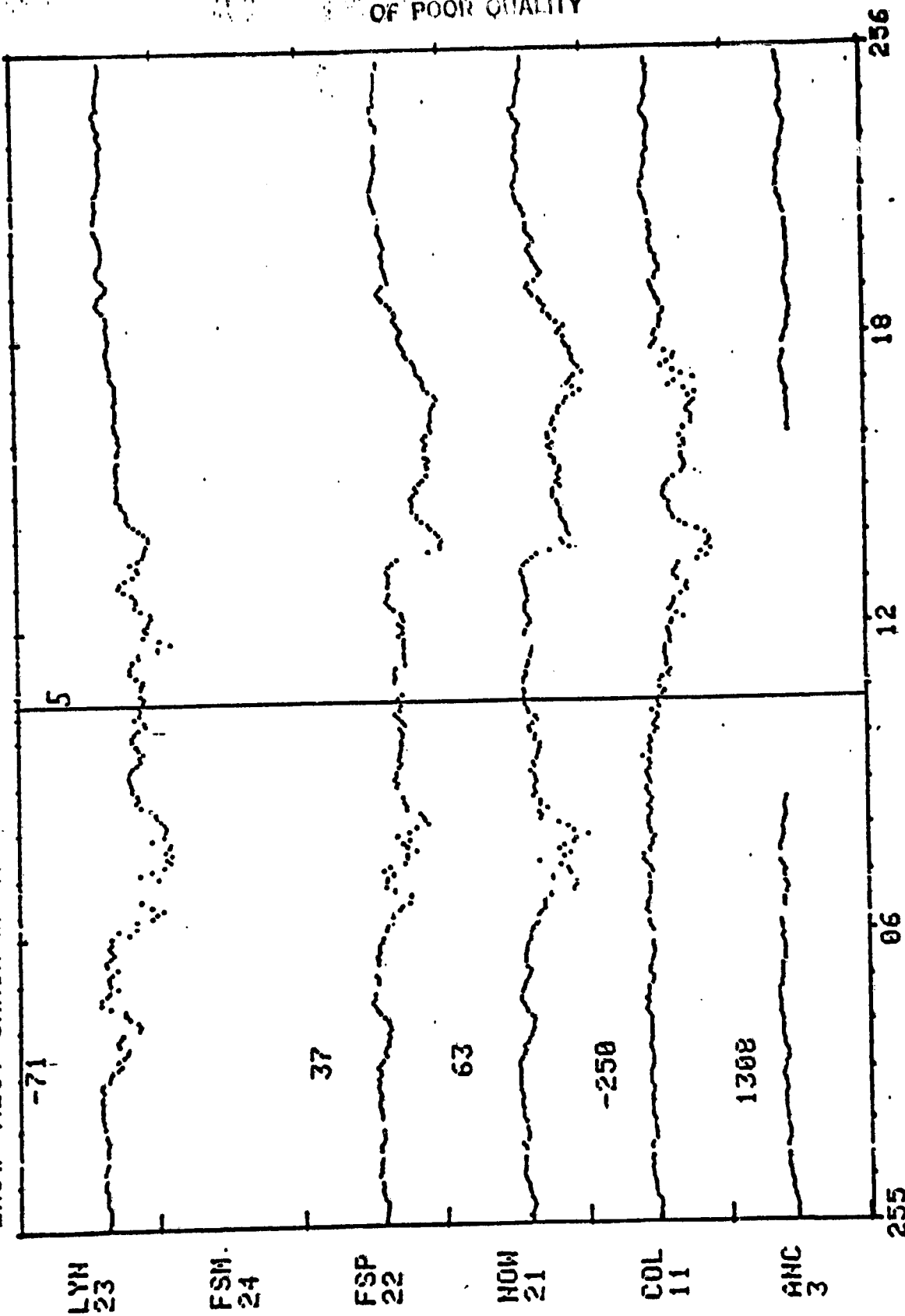


FIGURE 16

ORIGINAL PAGE IS  
OF POOR QUALITY

START TIME: 1981 283=1010 0000  
EAST-NEST CHAIN X TRACE TOTAL SCALE IS 5000 GAMMA

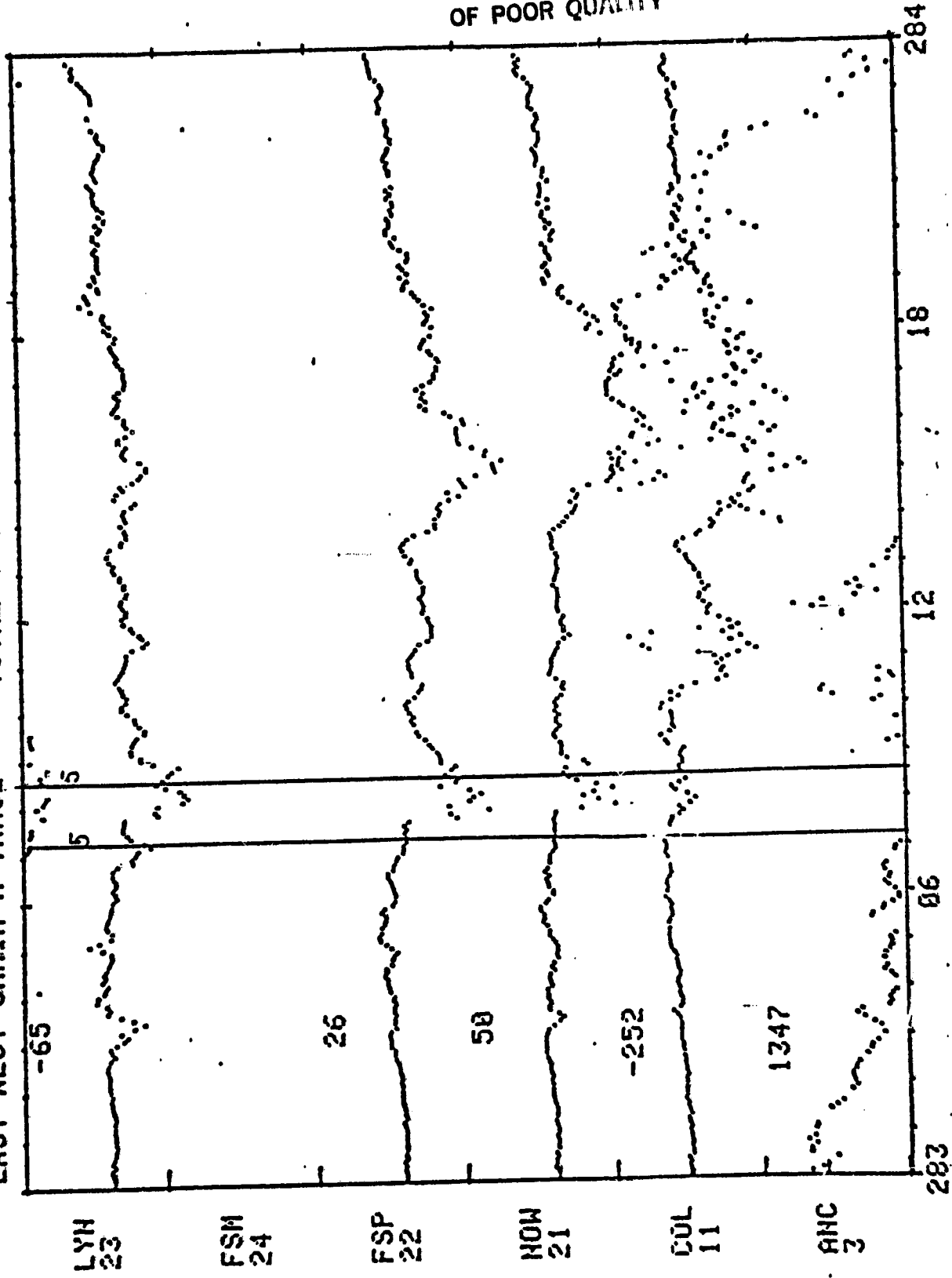


FIGURE 17

ORIGINAL PAGE IS  
OF POOR QUALITY

START TIME: 1981 204 10 11 0000  
EAST-NEST CHAIN X TRACE TOTAL SCALE IS 5000 GAMMA

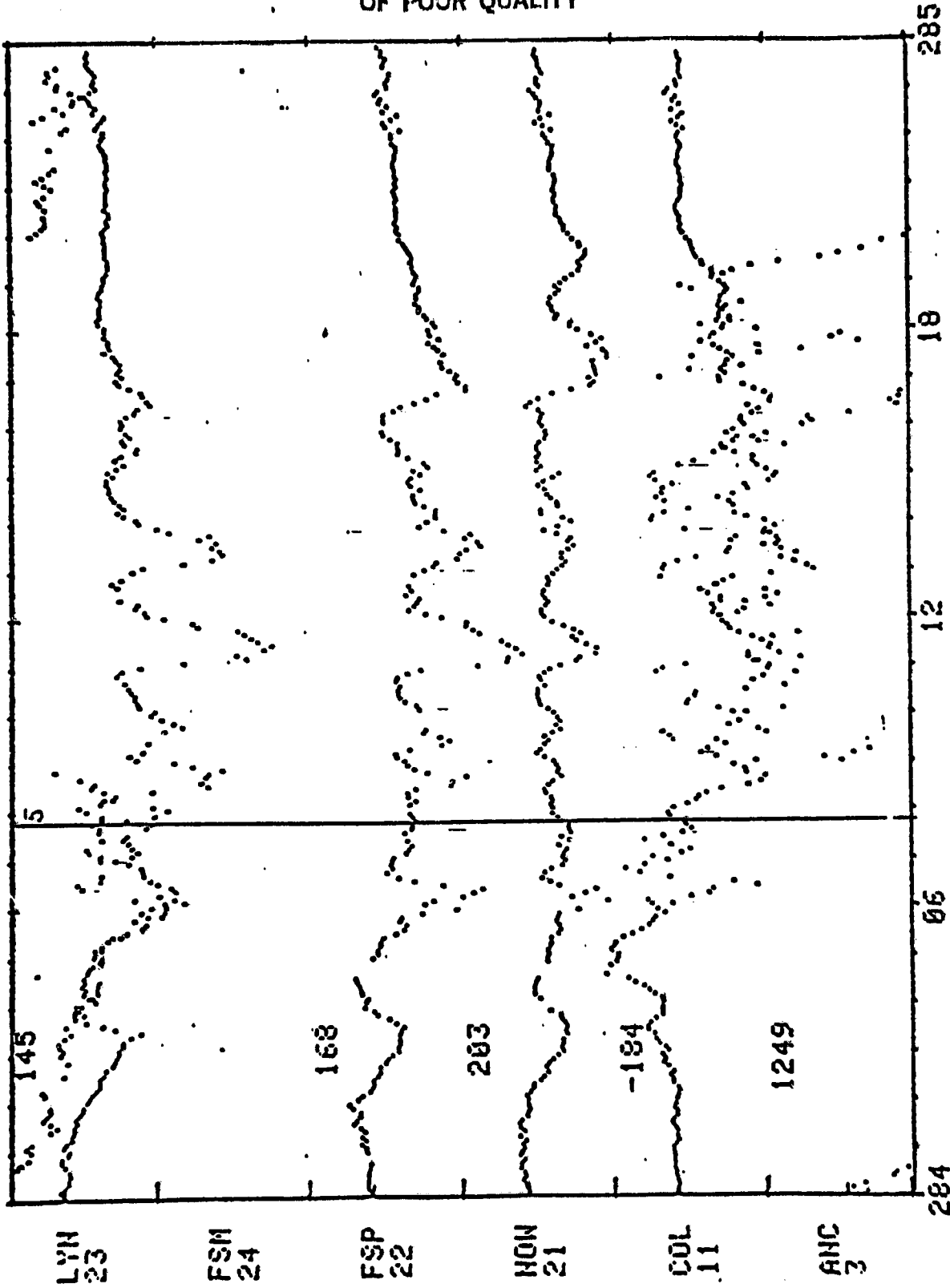
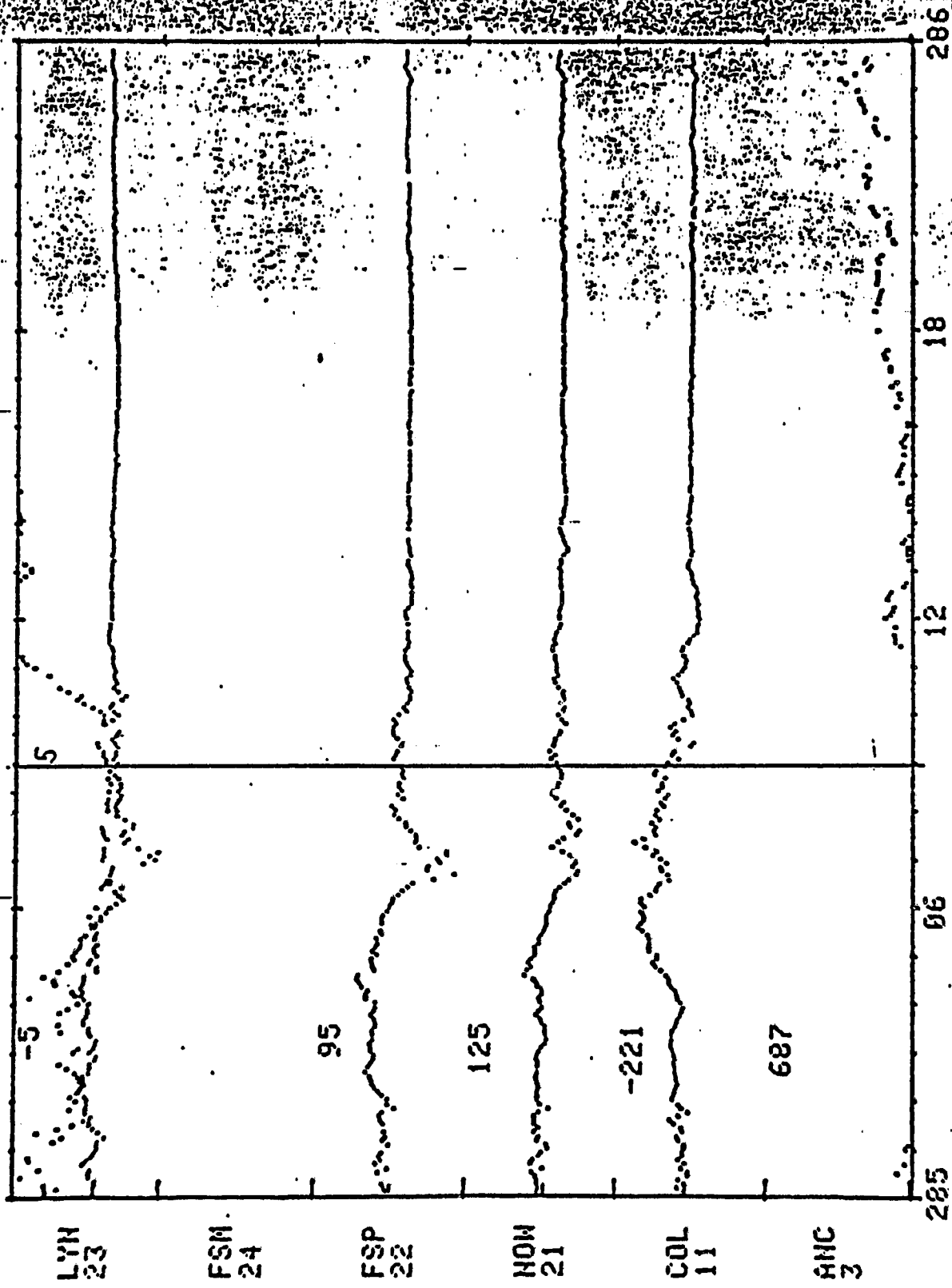


FIGURE 18



START TIME: 1981 285=1012 0000  
EAST-NEST CHAIN X TRACE TOTAL SCALE IS 5000 GAMMA



ORIGINAL PAGE IS  
OF POOR QUALITY

FIGURE 19

ORIGINAL PAGE IS  
OF POOR QUALITY

START TIME: 1981 294=1021 0000  
EAST-NEST CHAIN X TRACE TOTAL SCALE IS 5000 GAMMA

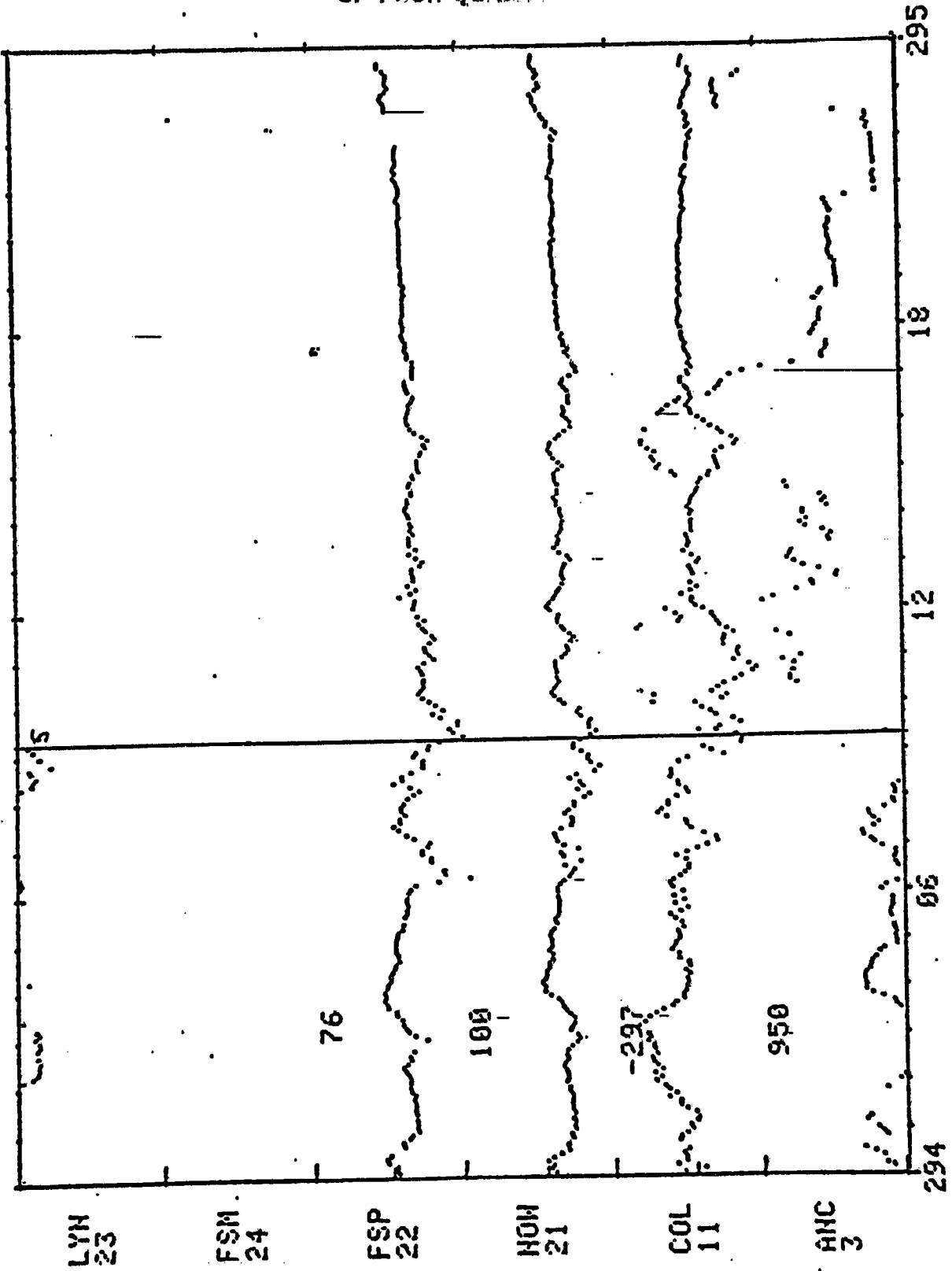


FIGURE 20

ORIGINAL PAGE IS  
OF POOR QUALITY

START TIME: 1981 316=1112 0000  
EAST-NEST CHAIN X TRACE TOTAL SCALE IS 5000 GAMMA

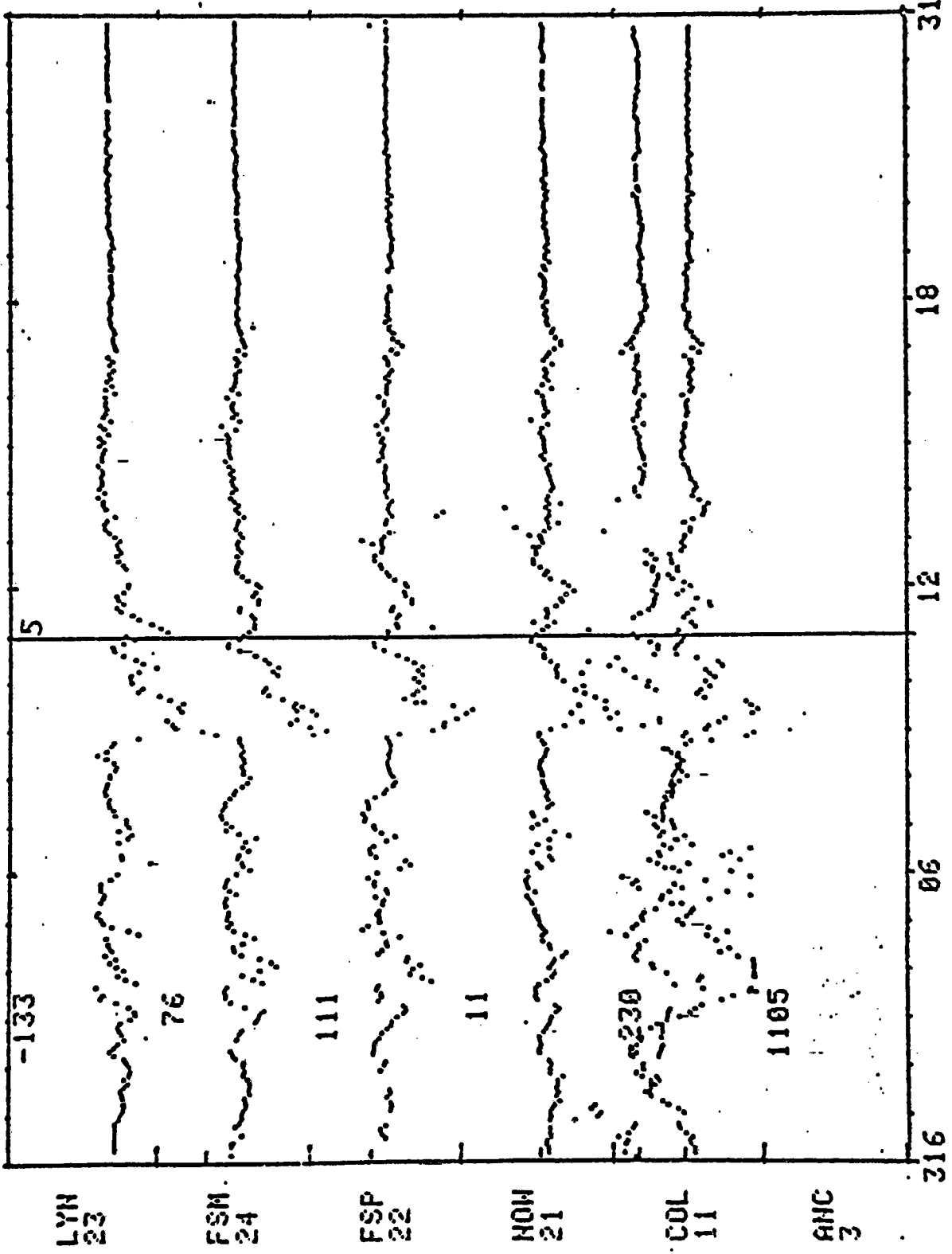


FIGURE 21

START TIME: 1981 326=1122 0000  
EAST-NEST CHAIN X TRACE TOTAL SCALE IS 5000 GAMMA

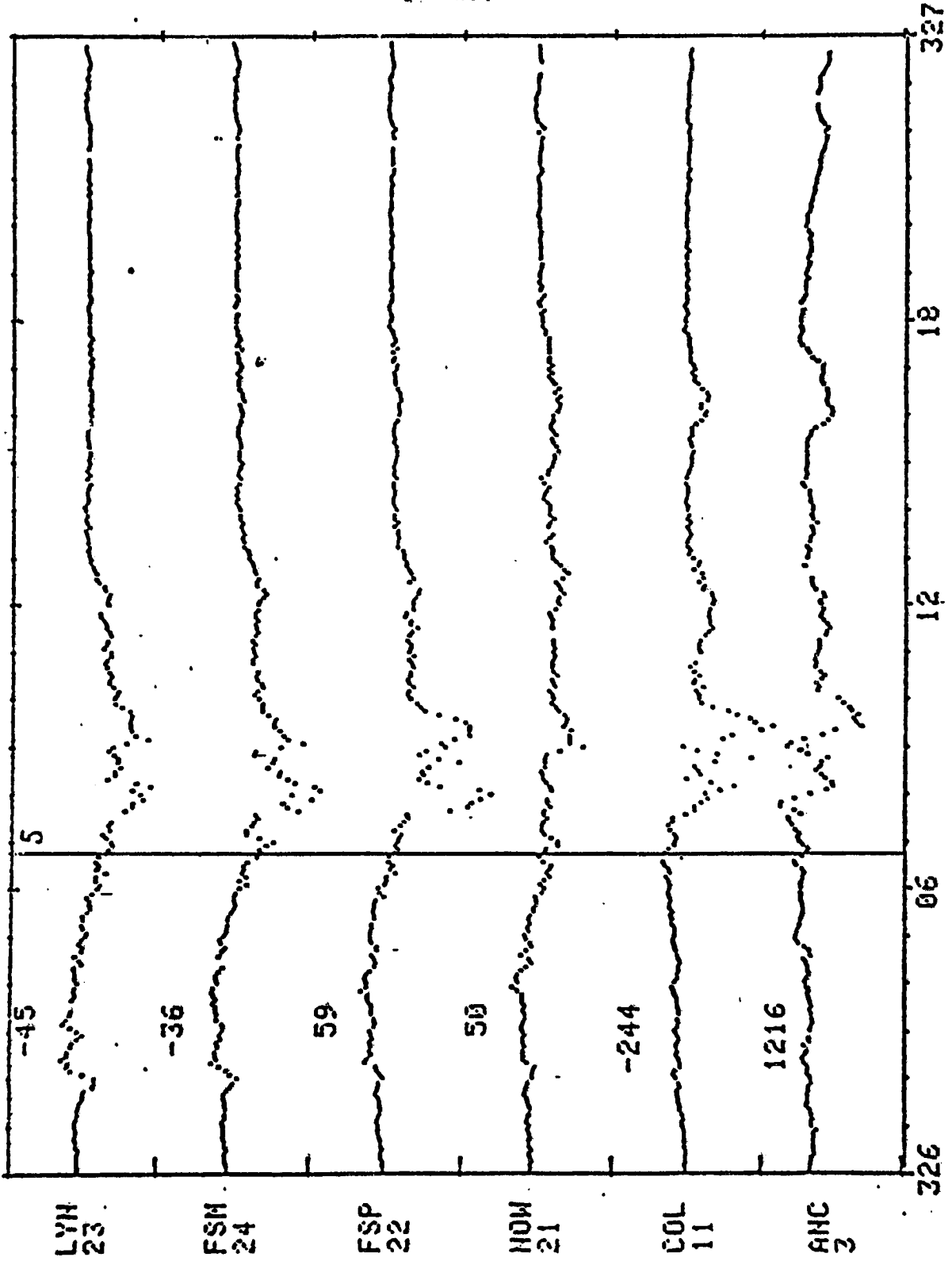


FIGURE 22

ORIGINAL PAGE IS  
OF POOR QUALITY

START TIME: 1981 327=1123 0000  
EAST-NEST CHAIN X TRACE TOTAL SCALE IS 5000 GAMMA

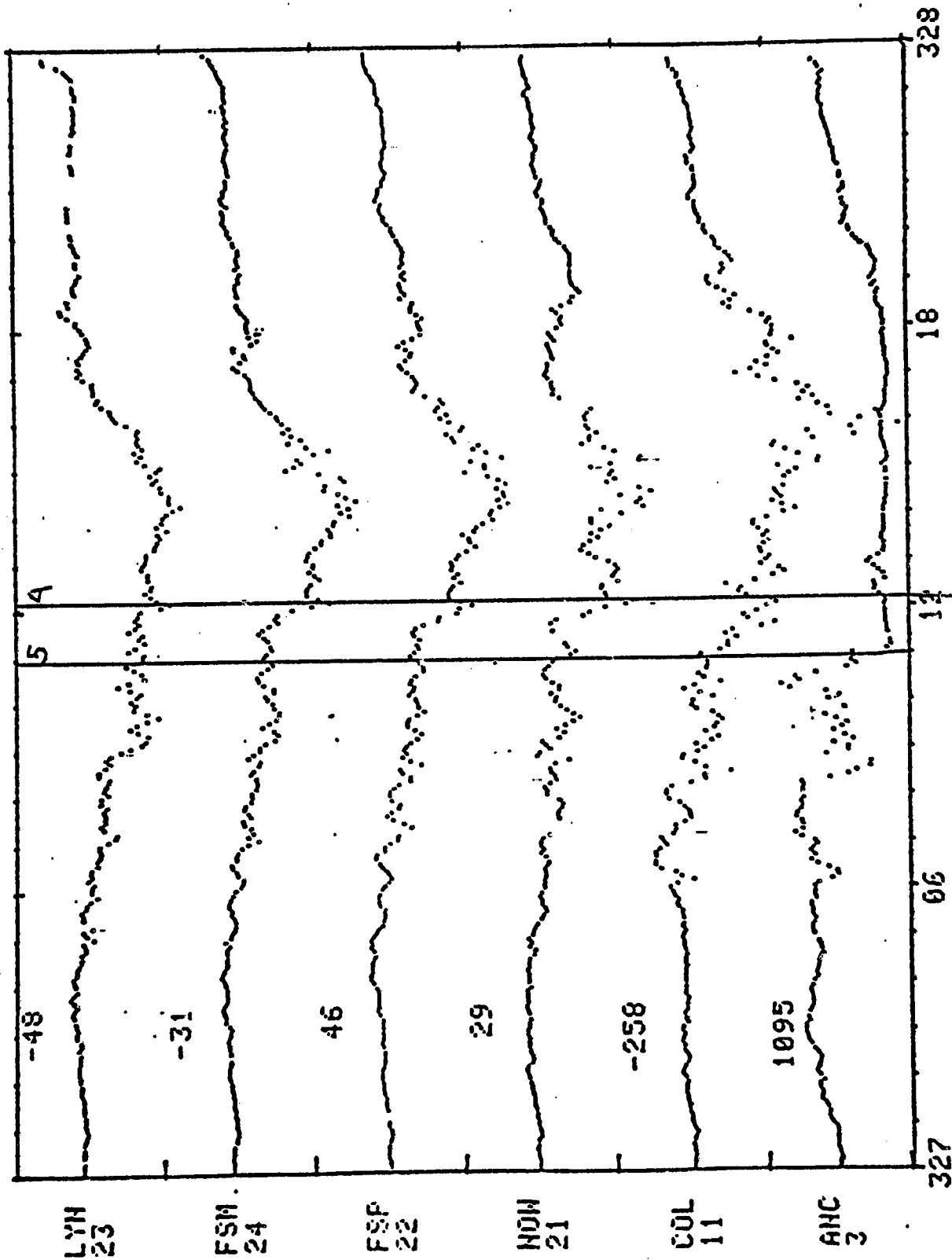


FIGURE 23

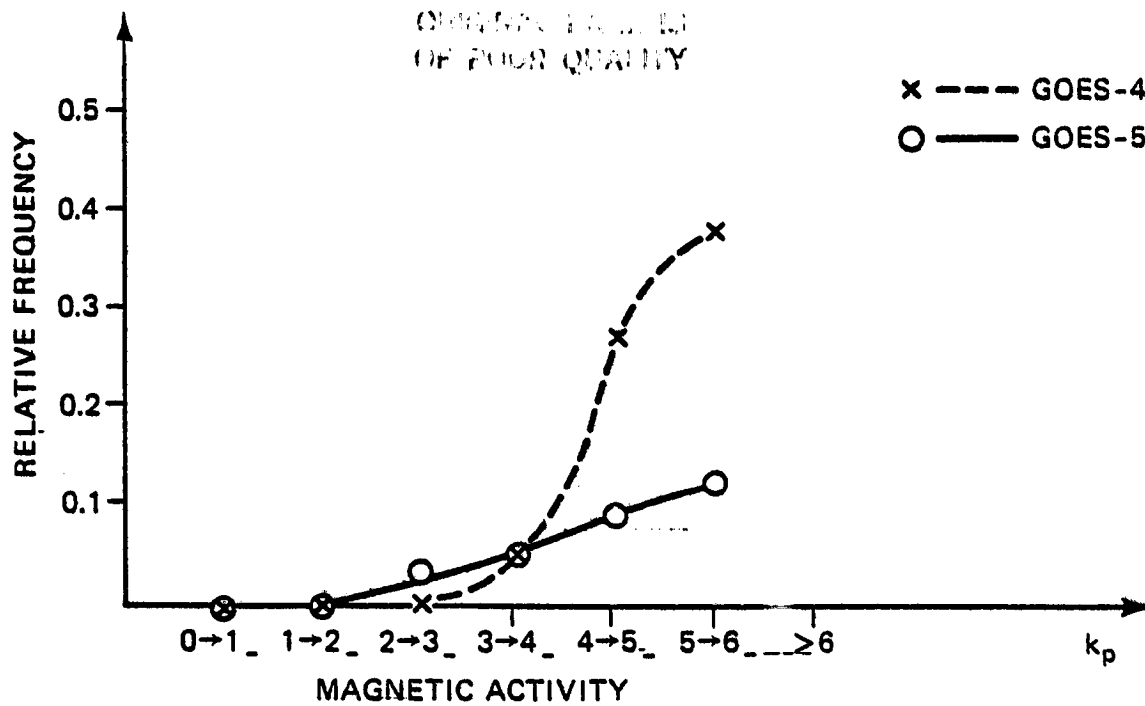


Figure 24. Relative Frequency of Anomalies

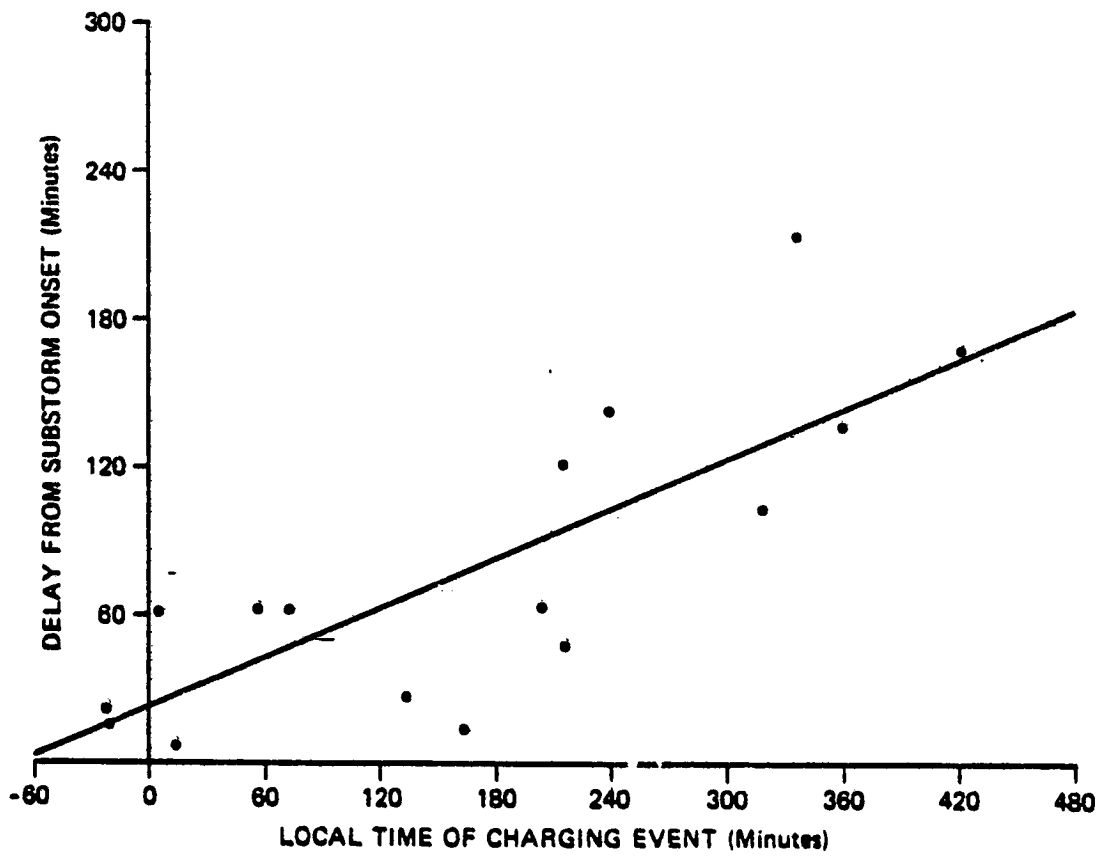


Figure 25. Plasma Drift Relationship